EPJ manuscript No.
(will be inserted by the editor)

The spectrum of interacting metallic carbon nanotubes: Exchange effects and universality

Leonhard Mayrhofer and Milena Grifoni

Theoretische Physik, Universität Regensburg, 93040 Regensburg, Germany

Received: date / Revised version: date

Abstract. The low energy spectrum of finite size metallic single-walled carbon nanotubes (SWNTs) is determined. Starting from a tight binding model for the p_z electrons, we derive the low energy Hamiltonian containing *all relevant scattering processes* resulting from the Coulomb interaction, including the short ranged contributions becoming relevant for small diameter tubes. In combination with the substructure of the underlying honeycomb lattice the short ranged processes lead to various exchange effects. Using bosonization the spectrum is determined. We find that the ground state is formed by a spin 1 triplet, if $4n+2$ electrons occupy the SWNT and the branch mismatch is smaller than the exchange splitting. Additionally, we calculate the excitation spectra for the different charge states and find the lifting of spin-charge separation as well as the formation of a quasi-continuum at higher excitation energies.

PACS. 73.63.Fg Nanotubes – 71.10.Pm Fermions in reduced dimensions – 71.70.Gm Exchange interactions

1 Introduction

Single walled carbon nanotubes (SWNTs) have remarkable mechanical and electronic properties. They represent, at low enough energies, an almost ideal realization of an one-dimensional (1D) electronic system with an additional orbital degree of freedom. Due to this 1D character the proper inclusion of the Coulomb interaction between the electrons in a SWNT is mandatory. For metallic SWNTs of infinite length the theoretical works [1,2] showed that correlations between the electrons can be described within the Luttinger liquid picture. The accompanying occurrence of power-laws for various transport properties could indeed be observed experimentally [3,4]. The effects of the forward scattering part of the electron-electron interactions in finite-size SWNTs were treated by Kane et al. in [5] within the bosonization framework. There the discrete energy spectrum of the collective spin and charge excitations was derived. The bosonization method has recently been used also to determine the transport properties of finite size metallic SWNT quantum dots [6].

So far the effect of non-forward scattering parts of the Coulomb interaction has only been discussed for SWNTs of infinite length by renormalization group techniques [1, 2]. In [1] deviations from conventional Luttinger Liquid behaviour have been found only for very small temperatures $T \lesssim 0.1$ mK provided that the interaction is long ranged. The work of Odintsov et al. [2] additionally took into account the situation at half filling where the formation of a Mott insulating state was predicted. In the works treating electron-electron interactions in finite size SWNTs within the bosonization formalism, the effect of non-forward scattering parts of the Coulomb interaction has been neglected. This approximation, which we will call "standard" theory in the following, is valid if moderate to large diameter tubes ($\gtrsim 1.5$ nm) are considered as in [5,6], or if finite size effects can be neglected since the relevant energies exceed the level spacing of the SWNT as in the experiments [3,4]. Recent experiments [7–9] however have found exchange effects in the ground state spectra of small diameter tubes which can not be explained using the "standard" bosonization theory for interacting SWNTs. Oreg et al. [10] have presented a mean-field Hamiltonian for the low energy spectrum of SWNTs including an exchange term favouring the spin alignment of electrons in different bands. The values for the exchange energies observed in the experiments agree well with the mean-field predictions. However, the question of a singlet-triplet ground state is beyond the mean field approach. Moreover, in contrast to the bosonization procedure it can not predict the strong energy renormalization of the charged collective electron excitations.

In this article we go beyond the mean-field approach. We derive a low-energy Hamiltonian for finite size metallic SWNTs, which includes *all* relevant short-ranged interaction processes. This allows us to identify the microscopic mechanisms that lead to the various exchange effects. Using bosonization we determine the spectrum and eigenstates of the SWNT Hamiltonian essentially exactly away from half-filling. An interesting situation arises near half-filling since there additional processes become relevant which can not be considered as small compared to the dominating forward scattering terms. Unfortunately

we have not found a reliable way of diagonalizing the Hamiltonian in that situation so far.

Concerning the ground state properties, we find under the condition of degenerate or almost degenerate bands, a spin 1 triplet as ground state if $4n+2$ electrons occupy the nanotube. This is insofar remarkable as a fundamental theorem worked out by Lieb and Mattis [11] states for any single-band Hubbard model in 1D with nearest-neighbour hopping that the ground state can only have spin 0 or 1/2. However at the end of their article they explicitly pose the question whether ground states with higher spin could be realized in 1D systems with orbital degeneracy, which in the case of SWNTs is present due to the substructure of the underlying honeycomb lattice. Our findings answer this question with yes, hence proofing that the theorem by Lieb and Mattis can not be generalized to multi-band systems. Moreover it is interesting to notice that all of the processes favouring higher spin states in SWNTs involve non-forward scattering with respect to the orbital degree of freedom. On the experimental side an exchange splitting in the low energy spectrum of the $4n+2$ charge state has indeed been observed [7–9]. However, all the experiments demonstrating exchange splitting were carried out for SWNTs with a large band mismatch such that the ground states are supposed to be spin 0 singlets. Especially Moriyama et al. have proven that this is the case in their experiments [9] by carrying out magnetic field measurements. Thus the threefold degenerate spin 1 ground state has not been observed yet, since its occurrence requires a band mismatch that is small compared to the exchange energy. Additionally to the ground state properties of metallic SWNTs we have also determined the excitation spectra. We find that the huge degeneracies as obtained by only retaining the forward scattering processes are partly lifted and the spectrum becomes more and more continuous when going to higher energies. Finally this leads to a lifting of the spin charge separation predicted by the "standard" theory.

The outline of this article is the following. We start in Section 2.1 by briefly reviewing the low energy physics of noninteracting electrons in finite size metallic SWNTs. Including the Coulomb interaction we derive the effectively one-dimensional Hamiltonian for the low energy regime in Section 2.2. The subsequent examination of the effective 1D interaction potential in Section 2.2.1 allows us to sort out the irrelevant interaction processes. The remaining processes are either of density-density or non-density-density form. The former ones we diagonalize together with the kinetic part of the Hamiltonian by bosonization in 3.1. Using the obtained eigenstates as basis we calculate the corresponding matrix elements for the non-density-density part of the interaction with the help of the bosonization identity of the electron operators, Section 3.2. In Section 4 we calculate the ground state and excitation spectra by diagonalizing the Hamiltonian including the non-density-density processes in a truncated basis and discuss the results.

For the hurried reader we propose to skip the more technical sections and, after reading Section 2, to go directly to Sections 4.1 and 4.2 where the results of this work are presented for the low energy and low to intermediate energy regions, respectively.

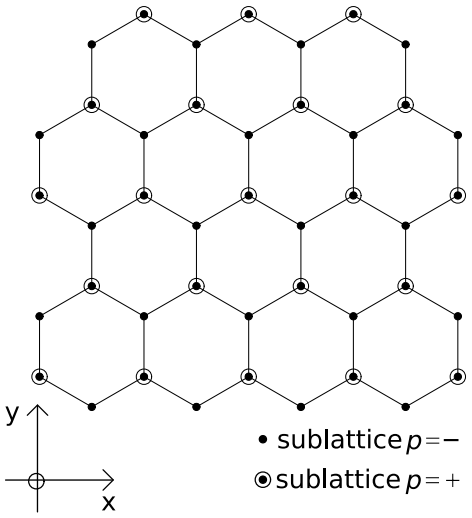

Fig. 1. The graphene lattice with its sublattice structure.

2 Low energy Hamiltonian of metallic finite size SWNTs

As shown in [12], correlation effects in metallic SWNTs are universal at low energies, i. e. they do not depend on the chirality of the considered tube. Therefore we can, without loss of generality, focus on armchair nanotubes from now on.

In this section we will give a short summary of the electronic structure of noninteracting finite size armchair nanotubes in the low energy regime following our earlier work [6]. On this basis we are going to include the Coulomb interaction between the electrons, leading to an effective 1D Hamiltonian. The subsequent examination of the effective 1D interaction potential will determine all the relevant scattering processes, which are either of density-density or non-density-density form.

2.1 The noninteracting System

Before considering the effect of the electron-electron interactions, let us recall the most important facts about noninteracting electrons in finite size armchair SWNTs. Since SWNTs can be considered as graphene sheets rolled up to cylinders, the bandstructure of SWNTs is easily derived from the one of the p_z electrons in the graphene honeycomb lattice, see e.g. [13]. Two carbon atoms $p = \pm$ occupy the unit cell of graphene, cf. Fig. 1, leading to a valence and a conduction band touching at the two Fermi points $F = \pm K_0 \hat{e}_x$. Quantization around the circumference of a SWNT restricts the set of allowed wave vectors, leading to the formation of subbands. For metallic SWNTs, only the

gapless subbands with linear dispersion, touching at the Fermi points, are relevant at low enough energies. Imposing open boundary conditions along the tube length L, the eigenfunctions of the noninteracting Hamiltonian H_0 are standing waves $\varphi_{r\kappa}(\boldsymbol{r})$ where the occurrence of the branch or pseudo spin index $r = \pm$ is a consequence of the double occupancy of the graphene unit cell. Furthermore κ measures the wave number relative to the Fermi wave number K_0 and is subject to the quantization condition

$$\kappa = \frac{\pi}{L}(n_\kappa + \Delta),\ n_\kappa \in \mathbb{Z},\ |\Delta| \leq 1/2. \tag{1}$$

The parameter Δ has to be introduced if there is no integer n with $K_0 = \pi n/L$, where L is the tube length, and is responsible for a possible energy mismatch ε_Δ between the $r = +$ and $r = -$ electrons. In general Δ depends also on the type of the considered SWNT [14]. Explicitly, $\varphi_{r\kappa}(\boldsymbol{r})$ can be decomposed into contributions from the two sublattices $p = \pm$,

$$\varphi_{r\kappa}(\boldsymbol{r}) = \frac{1}{\sqrt{2}} \sum_{p=\pm} f_{pr} \left(e^{i\kappa x} \varphi_{pK_0}(\boldsymbol{r}) - e^{-i\kappa x} \varphi_{p-K_0}(\boldsymbol{r}) \right). \tag{2}$$

The coefficients f_{pr} are given by

$$f_{pr} = \begin{cases} 1/\sqrt{2}, & p = + \\ -r/\sqrt{2}, & p = - \end{cases}, \tag{3}$$

and the functions φ_{pF} describe fast oscillating Bloch waves on sublattice p at the Fermipoint F,

$$\varphi_{pF}(\boldsymbol{r}) = \frac{1}{\sqrt{N_L}} \sum_{\boldsymbol{R}} e^{iFR_x} \chi(\boldsymbol{r} - \boldsymbol{R} - \boldsymbol{\tau}_p), \tag{4}$$

where N_L is the total number of lattice sites and $\chi(\boldsymbol{r} - \boldsymbol{R} - \boldsymbol{\tau}_p)$ is the p_z orbital localized on site $\boldsymbol{R}$ of sublattice p, see Fig. 1.

In Fig. 2 we show the linear dispersion relation for the standing waves $\varphi_{r\kappa}$. The slopes of the two branches are given by $r\hbar v_F$, with the Fermi velocity $v_F \approx 8.1 \cdot 10^5 m/s$. Including the spin degree of freedom, the Hamiltonian of the noninteracting system H_0 therefore reads

$$H_0 = \hbar v_F \sum_{r\sigma} r \sum_\kappa \kappa c^\dagger_{r\sigma\kappa} c_{r\sigma\kappa}, \tag{5}$$

where $c_{r\sigma\kappa}$ annihilates an electron in the state $|\varphi_{r\kappa}\rangle |\sigma\rangle$. Thus the level spacing of the noninteracting system is given by

$$\varepsilon_0 = \hbar v_F \frac{\pi}{L}. \tag{6}$$

In the next section we are going to express the interaction part of the Hamiltonian in terms of the 3D electron operators, which expressed in terms of the wave functions $\varphi_{r\kappa}(\boldsymbol{r})$ read

$$\Psi(\boldsymbol{r}) = \sum_\sigma \sum_{r\kappa} \varphi_{r\kappa}(\boldsymbol{r}) c_{r\sigma\kappa} =: \sum_\sigma \Psi_\sigma(\boldsymbol{r}).$$

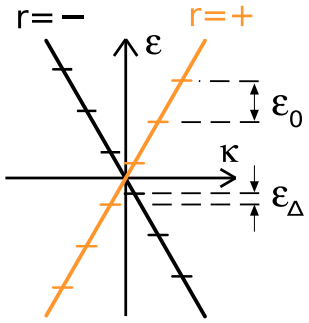

Fig. 2. The energy spectrum of a noninteracting metallic SWNT with the two branches $r = \pm$. The level spacing is denoted ε_0 and ε_Δ is the energy mismatch between $r = +$ and $r = -$.

By defining the slowly varying 1D electron operators,

$$\psi_{rF\sigma}(x) := \frac{1}{\sqrt{2L}} \sum_\kappa e^{i\mathrm{sgn}(F)\kappa x} c_{r\sigma\kappa},$$

we obtain with (2),

$$\Psi_\sigma(\boldsymbol{r}) = \sqrt{L} \sum_{rF} \mathrm{sgn}(F) \psi_{rF\sigma}(x) \sum_p f_{pr} \varphi_{pF}(\boldsymbol{r}). \tag{7}$$

2.2 The interaction Hamiltonian

In this section we examine the interaction part of the Hamiltonian. After introducing an effective 1D interaction potential, we discuss which of the scattering processes are of importance. We start with the general expression for the Coulomb interaction,

$$V = \frac{1}{2} \sum_{\sigma\sigma'} \int d^3r \int d^3r' \Psi^\dagger_\sigma(\boldsymbol{r}) \Psi^\dagger_{\sigma'}(\boldsymbol{r}') U(\boldsymbol{r} - \boldsymbol{r}') \Psi_{\sigma'}(\boldsymbol{r}') \Psi_\sigma(\boldsymbol{r}),$$

where $U(\boldsymbol{r} - \boldsymbol{r}')$ is the Coulomb potential. For the actual calculations we model $U(\boldsymbol{r} - \boldsymbol{r}')$ by the so called Ohno potential which interpolates between U_0, the interaction energy between two p_z electrons in the same orbital for $\boldsymbol{r} = \boldsymbol{r}'$ and $\frac{e^2}{4\pi\epsilon_0\epsilon|\boldsymbol{r} - \boldsymbol{r}'|}$ for large values of $|\boldsymbol{r} - \boldsymbol{r}'|$. Measuring distances in units of Å and energy in eV, it is given by [15]

$$U(\boldsymbol{r} - \boldsymbol{r}') = U_0 / \sqrt{1 + \left(U_0 \epsilon |\boldsymbol{r} - \boldsymbol{r}'| / 14.397 \right)^2}\, \mathrm{eV}. \tag{8}$$

A reasonable choice is $U_0 = 15$ eV [16]. The dielectric constant is given by $\epsilon \approx 1.4 - 2.4$ [1]. Reexpressing the 3D electron operators $\Psi_\sigma(\boldsymbol{r})$ in terms of the 1D operators $\psi_{rF\sigma}(x)$, cf. equation (7), and integrating over the coordinates perpendicular to the tube axis, we obtain,

$$V = \frac{1}{2} \sum_{\sigma\sigma'} \sum_{\{[r],[F]\}} \mathrm{sgn}(F_1F_2F_3F_4) \int dx \int dx' U_{[r][F]}(x, x') \times \psi^\dagger_{r_1F_1\sigma}(x) \psi^\dagger_{r_2F_2\sigma'}(x') \psi_{r_3F_3\sigma'}(x') \psi_{r_4F_4\sigma}(x), \tag{9}$$

where $\sum_{\{[r],[F]\}}$ denotes the sum over all quadruples $[r] = (r_1, r_2, r_3, r_4)$ and $[F] = (F_1, F_2, F_3, F_4)$. Under the assumption, justified by the localized character of the p_z orbitals, that the sublattice wave functions $\varphi_{pF}(\boldsymbol{r})$ and $\varphi_{-pF}(\boldsymbol{r})$ do not overlap, i.e., $\varphi_{pF}(\boldsymbol{r})\varphi_{-pF}(\boldsymbol{r}) \equiv 0$, the effective 1D Coulomb potential $U_{[r][F]}(x, x')$ is given by,

$$U_{[r][F]}(x,x') = L^2 \int d^2r_\perp \int d^2r'_\perp \sum_{p,p'} f_{pr_1} f_{p'r_2} f_{p'r_3} f_{pr_4} \times \varphi^*_{pF_1}(\boldsymbol{r})\varphi^*_{p'F_2}(\boldsymbol{r}')\varphi_{p'F_3}(\boldsymbol{r}')\varphi_{pF_4}(\boldsymbol{r})U(\boldsymbol{r}-\boldsymbol{r}'). \quad (10)$$

Using relation (3) for the coefficients f_{pr} and performing the sum over p, p', we can separate $U_{[r][F]}$ into a part describing the interaction between electrons living on the same (intra) and on different (inter) sublattices,

$$U_{[r][F]}(x,x') = \frac{1}{4}\Big[U^{intra}_{[F]}(x,x')(1 + r_1r_2r_3r_4) + U^{inter}_{[F]}(x,x')(r_2r_3 + r_1r_4)\Big], \quad (11)$$

where

$$U^{intra/inter}_{[F]}(x,x') = L^2 \int\int d^2r_\perp d^2r'_\perp \times \varphi^*_{pF_1}(\boldsymbol{r})\varphi^*_{\pm pF_2}(\boldsymbol{r}')\varphi_{\pm pF_3}(\boldsymbol{r}')\varphi_{pF_4}(\boldsymbol{r})U(\boldsymbol{r}-\boldsymbol{r}'). \quad (12)$$

Note that the 3D extention of the considered SWNT enters the effective 1D interaction potential via equation (12). In Appendix A we show how we actually determine the values for the potentials $U^{intra/inter}_{[F]}(x,x')$.

2.2.1 The relevant scattering processes

Not all of the terms in (9) contribute to the interaction because the corresponding potential $U_{[r][F]}$ vanishes or has a very small amplitude. In order to pick out the relevant terms, it is convenient to introduce the notion of forward (f)-, back (b)- and Umklapp (u)- scattering with respect to an arbitrary index quadruple $[I]$ associated to the electron operators in (9). Denoting the scattering type by S_I we write $[I]_{S_I=f^\pm}$ for $[I, \pm I, \pm I, I]$. Furthermore we use $[I]_{S_I=b}$ for $[I, -I, I, -I]$ and $[I]_{S_I=u}$ is equivalent to $[I, I, -I, -I]$, cf. Fig. 3. Keeping only the relevant terms, the interaction part of the Hamiltonian acquires the form,

$$V = \sum_{S_r=f,b,u} \sum_{S_F=r,b} \sum_{S_\sigma=f} V_{S_rS_FS_\sigma}, \quad (13)$$

where

$$V_{S_rS_FS_\sigma} := \frac{1}{2} \sum_{\{[r]_{S_r},[F]_{S_F},[\sigma]_{S_\sigma}\}} \int\int dx\, dx' U_{[r][F]}(x,x') \times \psi^\dagger_{r_1F_1\sigma}(x)\psi^\dagger_{r_2F_2\sigma'}(x')\psi_{r_3F_3\sigma'}(x')\psi_{r_4F_4\sigma}(x), \quad (14)$$

as we are going to demonstrate in the following.

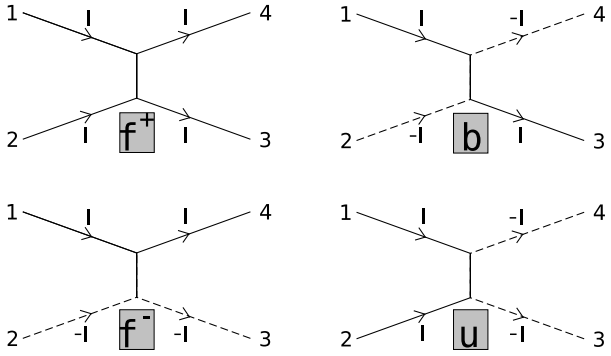

Fig. 3. The relevant scattering processes. Forward/back/Umklapp scattering are denoted by $f^\pm/b/u$. The index I represents one of the three degrees of freedom r, F, σ (branch, Fermi point and spin, respectively).

Scattering of r We start with the possible scattering events related to the pseudo spin r. From (11) we can immediately read off that the interaction potential $U_{[r][F]}$ does not vanish only if $r_2r_3 = r_1r_4$. Thus we find the following cases for the relevant scattering types,

$$i)\ r_1 = r_4,\ r_2 = r_3 \text{ and } ii)\ r_1 = -r_4,\ r_2 = -r_3.$$

Relation $i)$ summarizes all the forward scattering processes with respect to r and the associated interaction potential is,

$$U_{[r]_f[F]}(x,x') = \frac{1}{2}\Big[U^{intra}_{[F]}(x,x') + U^{inter}_{[F]}(x,x')\Big] =: U^+_{[F]}(x,x'). \quad (15)$$

Case $ii)$ includes all $S_r = b$ and $S_r = u$ processes and here the interaction potential is proportional to the difference between U^{intra} and U^{inter},

$$U_{[r]_{b/u}[F]}(x,x') = \frac{1}{2}\Big[U^{intra}_{[F]}(x,x') - U^{inter}_{[F]}(x,x')\Big] =: U^\Delta_{[F]}(x,x'). \quad (16)$$

Scattering of F The determination of the essential scattering processes with respect to F can be achieved by exploiting the approximate conservation of quasi momentum. Looking at expression (4) for the wave functions $\varphi_{pF}(\boldsymbol{r})$, we find that the interaction potential $U_{[r][F]}$, cf. (10), contains phase factors of the form $e^{-i(F_1-F_4)R_x} \times e^{-i(F_2-F_3)R'_x}$. Although we are considering a finite system, therefore not having perfect translational symmetry, after the integration along the tube axis in (9), only terms without fast oscillations survive [1]. The corresponding condition is given by

$$F_1 - F_4 + F_2 - F_3 = 0, \quad (17)$$

[1] For a perfectly translational invariant 1D system it holds

that means only the $S_F = f$ and $S_F = b$ terms survive. We have explicitly checked that due to the discrete nature of the SWNT lattice also the $S_F = u$ processes have very small amplitudes and can be neglected. Note that condition (17) leads to $\mathrm{sgn}(F_1F_2F_3F_4) = 1$ in (9).

Scattering of σ It is clear that only $S_\sigma = f$ processes are allowed, since the Coulomb interaction is spin independent.

Altogether this proofs equation (13).

Processes conserving or not conserving the fermionic configuration From the discussion in Section 2.1 we already know that we have to distinguish between electrons with different spin σ and pseudo spin r. In the following we will denote the number of electrons of a certain species by $N_{r\sigma}$ and we will refer to the quantity $\boldsymbol{N} = (N_{+\uparrow}, N_{+\downarrow}, N_{-\uparrow}, N_{-\downarrow})$ as fermionic configuration. Not all of the scattering processes in (13) conserve $\boldsymbol{N}$. In more detail, for terms with $(S_r, S_\sigma) = (u, f^+)$, $(S_r, S_\sigma) = (b, f^-)$ and $(S_r, S_\sigma) = (u, f^-)$ $\boldsymbol{N}$ is not a good quantum number as can be easily verified by using equation (14). In general, only processes described by the $\boldsymbol{N}$ conserving terms are sensitive to the total number of electrons in the dot. As example we mention the charging energy contribution proportional to N_c^2, $N_c := \sum_{r\sigma} N_{r\sigma}$ arising from the $(S_r, S_F, S_\sigma) = (f, f, f)$ processes appearing later on. On the other hand for the $\boldsymbol{N}$ non conserving terms, only the vicinity of the Fermi surface is of relevance.

Processes only relevant near half-filling Away from half-filling we find that terms with

$$r_1F_1 + r_2F_2 - r_3F_3 - r_4F_4 \neq 0, \tag{18}$$

i.e., the Umklapp scattering terms with respect to the product rF [2] can be neglected in (9). For the $\boldsymbol{N}$ non conserving terms fulfilling (18) this is a consequence of the approximate conservation of quasi momentum, arising from the slow oscillations of the 1D electron operators in (14) which near the Fermi surface are given by the exponential $e^{-i\left[\left(r_1F_1N_{r_1\sigma_1} - r_4F_4N_{r_4\sigma_4}\right)x + \left(r_2F_2N_{r_2\sigma_2} - r_3F_3N_{r_3\sigma_3}\right)x'\right]}$. After performing the integrations in (14) this leads approximately to (18). The $\boldsymbol{N}$ conserving terms obeying (18), V_{f^-bf} and $V_{bf^-f^+}$, which describe not only processes near the Fermi level, add a term proportional to the number of electrons above half-filling to the Hamiltonian, therefore just giving rise to a shift of the chemical potential.

$$\int_0^L dx' \int_0^L dx\, U(x-x') e^{ikx} e^{ik'x'} = \int_0^L dx' \int_{-x'}^{L-x'} dy\, U(y) e^{iky} e^{i(k+k')x'} = \tilde{U}_k \int_0^L dx' e^{i(k+k')x'},$$

where $\tilde{U}_k = \int_{-x'}^{L-x'} dy U(y) e^{iky}$ does not depend on x' because we have assumed translational invariance. So it is clear that the double integral vanishes unless $k + k' \approx 0$.

[2] There are simple rules for determining the scattering type S_{rF} if S_r and S_F are known. Defining a product by $S_{rF} = S_rS_F = S_FS_r$ it holds, $Sf^+ = S$; $S^2 = f^+$; $f^-u = b$; $f^-b = u$ and $ub = f^-$.

	$\frac{u^+ d}{\varepsilon_0}$	$\frac{u_f^\Delta d}{\varepsilon_0}$	$\frac{u_b^\Delta d}{\varepsilon_0}$
$\epsilon = 1.4$	0.22Å	0.14Å	0.22Å
$\epsilon = 2.4$	0.28Å	0.22Å	0.28Å

Table 1. The dependence of the coupling constants u^+, u_f^Δ and u_b^Δ on the tube diameter d and on the dielectric constant ϵ.

2.2.2 Long ranged vs. short ranged interactions

Except of $U_{[r]_f[F]_f} = U^+_{[F]_f}$, all relevant interaction potentials $U_{[r][F]}$ can effectively be treated as local interactions: In the case of $U^+_{[F]_b}$ this is due to the appearance of phase factors $e^{i2F(R_x - R'_x)}$ in (12), arising from the Bloch waves $\varphi_{pF}(\boldsymbol{r})$, cf. equation (4), oscillating much faster than the electron operators $\psi_{r\sigma F}(x)$. The potentials $U^\Delta_{[F]}$, being proportional to the difference of the inter- and intra-lattice interaction potentials, are in general short ranged, since $U^{intra}_{[F]}(x,x')$ and $U^{inter}_{[F]}(x,x')$ only have considerably differing values for $|x - x'| \lesssim a_0$ with the next neighbour distance $a_0 = 0.142$ nm of the carbon atoms in the SWNT lattice [1]. Summarizing, *only the processes with $(S_r, S_F) = (f, f)$ are long ranged.* All other terms can effectively be written as local interactions. I.e. for $(S_r, S_F) \neq (f, f)$ we can use the approximation

$$\frac{1}{2} U_{[r]_{S_r}[F]_{S_F}}(x,x') \approx L u_{S_r\, S_F} \delta(x - x'), \tag{19}$$

where we have introduced the coupling parameters

$$u^{S_r\, S_F} := 1/(2L^2) \int\int dx\, dx' U_{[r]_{S_r}[F]_{S_F}}(x,x'). \tag{20}$$

Using the approximation (19) we obtain from (14) in the case $(S_r, S_F) \neq (f, f)$ the following expression for the non forward scattering interaction terms,

$$V_{S_rS_FS_\sigma} \approx L u_{S_r\, S_F} \sum_{\{[r]_{S_r}, [F]_{S_F}, [\sigma]_f\}} \times \int_0^L dx \psi^\dagger_{r_1F_1\sigma}(x) \psi^\dagger_{r_2F_2\sigma'}(x) \psi_{r_3F_3\sigma'}(x) \psi_{r_4F_4\sigma}(x). \tag{21}$$

In the following we use the abbreviations $u^+ := u_{f\,b}$ and $u^\Delta_{S_F} := u_{b\,S_F} = u_{u\,S_F}$. For details about the calculation, see Appendix A. We find that in general the coupling constants u^+ and $u^\Delta_{S_F}$ scale inversely with the total number of

lattice sites, i.e., like $1/Ld$, where d is the tube diameter. From a physical point of view this is due to an increasing attenuation of the wave functions for a growing system size. Therefore the probability of processes mediated by local interactions is proportional to $1/Ld$. Because the level spacing of the noninteracting system ε_0 scales like $1/L$, cf. (6), the products $u^+ d/\varepsilon_0$ and $u^{\Delta}_{S_F} d/\varepsilon_0$ are constants. The corresponding numerical values for different dielectric constants ϵ, cf. equation (8), are given in table 1.

2.2.3 Density-density vs. non-density-density processes

The interaction processes can be divided into density-density terms, easily diagonalizable by bosonization [17], and non-density-density terms respectively. It is clear that the forward scattering interaction $V_{f\,f\,f}$ is of density-density form,

$$V_{f\,f\,f} = \frac{1}{2}\sum_{rr'}\sum_{FF'}\sum_{\sigma\sigma'}\int\int dx\,dx' U^{+}_{[F]_f}(x,x') \times \rho_{rF\sigma}(x)\rho_{r'F'\sigma'}(x'), \quad (22)$$

where the densities $\rho_{rF\sigma}(x)$ are given by

$$\rho_{rF\sigma}(x) = \psi^{\dagger}_{rF\sigma}(x)\psi_{rF\sigma}(x).$$

But since we treat the short ranged interactions as local, also $V_{f^+\,b\,f^+}$,

$$V_{f^+\,b\,f^+} = Lu^+\sum_{r\sigma F}\int_0^L dx \psi^{\dagger}_{rF\sigma}(x)\psi^{\dagger}_{r-F\sigma}(x)\psi_{rF\sigma}(x)\psi_{r-F\sigma}(x) = -Lu^+\sum_{r\sigma F}\int_0^L dx \rho_{rF\sigma}(x)\rho_{r-F\sigma}(x), \quad (23)$$

and similarly $V_{b\,f^+/b\,f^+}$,

$$V_{b\,f^+/b\,f^+} = -Lu^{\Delta}_{f^+/b}\sum_{r\sigma F}\int_0^L dx \rho_{rF\sigma}(x)\rho_{-r\pm F\sigma}(x), \quad (24)$$

are density-density interactions. In total the density-density part of the interaction is given by

$$V_{\rho\rho} = V_{f\,f\,f} + V_{f^+\,b\,f^+} + V_{b\,f^+\,f^+} + V_{b\,b\,f^+}. \quad (25)$$

The remaining terms are not of density-density form and are collected in the operator $V_{\mathrm{n}\rho\rho}$. Including only the contributions relevant away from half-filling, we obtain,

$$V_{\mathrm{n}\rho\rho} = V_{f^+\,b\,f^-} + V_{b\,f^+\,f^-} + V_{b\,b\,f^-} + V_{u\,f^-\,f} + V_{u\,b\,f}. \quad (26)$$

Near half-filling additionally the processes

$$V_{f^-\,b\,f}, V_{b\,f^-\,f} \text{ and } V_{u\,f^+\,f^-}, \quad (27)$$

satisfying condition (18), contribute to $V_{n\rho\rho}$. Overall, the SWNT Hamiltonian acquires the form,

$$H = H_0 + V_{\rho\rho} + V_{\mathrm{n}\rho\rho}.$$

3 Expressing the SWNT Hamiltonian in the eigenbasis of $H_0 + V_{\rho\rho}$

Away from half-filling, the interaction is dominated by $V_{f\,f\,f}$. Together with H_0 it yields the "standard" theory for interacting electrons in SWNTs [1,2,5]. Using bosonization we will in the next step diagonalize $H_0 + V_{\rho\rho}$. Subsequently we will examine the effect of $V_{\mathrm{n}\rho\rho}$ by calculating the matrix elements of $V_{\mathrm{n}\rho\rho}$ between the eigenstates of $H_0 + V_{\rho\rho}$. The diagonalization of $V_{\mathrm{n}\rho\rho}$ in a truncated eigenbasis of $H_0 + V_{\rho\rho}$, discussed in Section 4 then yields to a good approximation the correct eigenstates and the spectrum of the total Hamiltonian H.

3.1 Diagonalizing $H_0 + V_{\rho\rho}$

By introducing operators creating/annihilating bosonic excitations we can easily diagonalize $H_0 + V_{\rho\rho}$ as we show in this section. It turns out that the Fourier coefficients of the density operators $\rho_{r\sigma F}(x)$ are essentially of bosonic nature. In detail, we get by Fourier expansion,

$$\rho_{rF\sigma}(x) = \frac{1}{2L}\sum_q e^{i\mathrm{sgn}(F)qx}\rho_{r\sigma q}, \quad (28)$$

where $q = \frac{\pi}{L}n_q$, $n_q \in \mathbb{Z}$. Then the operators $b_{\sigma q_r}$ defined by,

$$b_{\sigma q_r} := \frac{1}{\sqrt{n_q}}\rho_{r\sigma q_r}, \quad q_r := r\cdot q, \quad q>0 \quad (29)$$

fulfill the canonical commutation relations $[b_{\sigma q}, b^{\dagger}_{\sigma' q'}] = \delta_{\sigma'\sigma}\delta_{qq'}$ as shown e.g. in [17]. For completeness we give the explicit expression for $b_{\sigma q_r}$, $r=\pm$,

$$b_{\sigma q_r} = \frac{1}{\sqrt{n_q}}\sum_{\kappa} c^{\dagger}_{r\sigma\kappa}c_{r\sigma\kappa+q_r}, \quad q>0.$$

The bosonized expression for H_0 is well known [6],

$$H_0 = \sum_{r\sigma}\left[\varepsilon_0\sum_{q>0}|n_q|\, b^{\dagger}_{\sigma q_r}b_{\sigma q_r} + \frac{\varepsilon_0}{2}\mathcal{N}^2_{r\sigma} + r\frac{\varepsilon_{\Delta}}{2}\mathcal{N}_{r\sigma}\right], \quad (30)$$

Here the first term describes collective particle-hole excitations, whereas the second term is due to Pauli's principle and represents the energy cost for the shell filling. The third term accounts for a possible energy mismatch between the bands $r=\pm$, given by

$$\varepsilon_{\Delta} = \mathrm{sgn}(\Delta)\varepsilon_0\min(2|\Delta|, |2|\Delta| - 1|).$$

The operators $\mathcal{N}_{r\sigma}$ count the number of electrons $N_{r\sigma}$ in branch $(r\sigma)$. Bosonization of $V_{\rho\rho}$ can be achieved by inserting the Fourier expansion (28) into expressions (22), (23) and (24), thereby making use of definition (29). We

obtain,

$$V_{\rho\rho} = V_{f\,f\,f} + V_{f^+\,b\,f^+} + V_{b\,f^+/b\,f^+} = \frac{1}{2}\sum_{q>0} n_q \left\{ W_q \left[\sum_{r\sigma} \left(b_{\sigma r\cdot q} + b^\dagger_{\sigma r\cdot q} \right) \right]^2 - u^+ \sum_{r\sigma} \left(b_{\sigma r\cdot q} b_{\sigma r\cdot q} + h.c. \right) - u^\Delta_f \sum_{r\sigma} \left(b_{\sigma r\cdot q} b_{\sigma -r\cdot q} + h.c. \right) - u^\Delta_b \sum_{r\sigma} \left(b_{\sigma r\cdot q} b^\dagger_{\sigma -r\cdot q} + h.c. \right) \right\} + \frac{1}{2}\left[E_c \mathcal{N}_c^2 - \frac{J}{2} \sum_{r\sigma} \mathcal{N}_{r\sigma}\mathcal{N}_{-r\sigma} - u^+ \sum_{r\sigma} \mathcal{N}^2_{r\sigma} \right], \quad (31)$$

where the coefficients W_q determine the interaction strength of $V_{f\,f\,f}$ and are given by

$$W_q = \frac{1}{L^2} \int dx \int dx' U^+_{[F]_f}(x,x') \cos(qx)\cos(qx').$$

The last line of (31) describes the contribution of $V_{\rho\rho}$ to the system energy depending on the number of electrons in the single branches $(r\sigma)$. Here $E_c = W_0$ is the SWNT charging energy, $\mathcal{N}_c = \sum_{r\sigma} \mathcal{N}_{r\sigma}$ counts the total number of electrons. Spin alignment of electrons with different branch index r is favoured by the term proportional to $J/2 := u^\Delta_f + u^\Delta_b$. Finally the term coupling with u^+ counteracts the energy cost for the shell filling in equation (30).

Since the bosonic operators appear quadratically in (30) and (31) we can diagonalize $H_0 + V_{\rho\rho}$ by introducing new bosonic operators $a_{j\delta q}$ and $a^\dagger_{j\delta q}$ via the Bogoliubov transformation [18] given below by equation (33). We obtain

$$H_0 + V_{\rho\rho} = \sum_{j\delta} \sum_{q>0} \varepsilon_{j\delta q} a^\dagger_{j\delta q} a_{j\delta q} + \frac{1}{2} E_c \mathcal{N}_c^2 + \frac{1}{2} \sum_{r\sigma} \mathcal{N}_{r\sigma} \left[-\frac{J}{2} \mathcal{N}_{-r\sigma} + \left(\varepsilon_0 - u^+ \right) \mathcal{N}_{r\sigma} + r\varepsilon_\Delta \right]. \quad (32)$$

The first term describes the bosonic excitations of the system, created/annihilated by the operators $a^\dagger_{j\delta q}$ / $a_{j\delta q}$. The four channels $j\delta = c+, c-, s+, s-$ are associated to total $(+)$ and relative $(-)$ (with respect to the index r) spin (s) and charge (c) excitations. The decoupling of the four modes $j\delta$, the so called spin-charge separation, will be partly broken by $V_{\mathrm{n}\rho\rho}$. The excitation energies $\varepsilon_{j\delta q}$ and the relation between the new bosonic operators $a_{j\delta q}$ and the old operators $b_{\sigma q_r}$ are determined by the Bogoliubov transformation. In detail, we find with $\varepsilon_{0q} := \varepsilon_0 n_q$,

$$\varepsilon_{c+q} = \varepsilon_{0q}\sqrt{1 + 8W_q/\varepsilon_0},$$

$$\varepsilon_{s/c-q} = \varepsilon_{0q}(1 - u^\Delta_b/\varepsilon_0)$$

and

$$\varepsilon_{s+q} = \varepsilon_{0q}(1 + u^\Delta_b/\varepsilon_0).$$

The energies of the $c+$ channel are largely enhanced compared to the other excitations because of the dominating $V_{f\,f\,f}$ contribution. For small q the ratio $g_q := \varepsilon_{0q}/\varepsilon_{c+q}$ is approximately 0.2, whereas for large q it tends to 1 [6]. Small corrections due to the coupling constants u^Δ_f and u^+ have been neglected. For the transformation from the old bosonic operators $b_{\sigma q_r}$ to the new ones $a_{j\delta q}$ we find

$$b_{\sigma q_r} = \sum_{j\delta} \Lambda^{j\delta}_{r\sigma} \left(B_{j\delta q} a_{j\delta q} + D_{j\delta q} a^\dagger_{j\delta q} \right), \quad q > 0 \quad (33)$$

where

$$\Lambda^{j\delta}_{r\sigma} = \frac{1}{2} \begin{pmatrix} 1 & 1 & 1 & 1 \\ 1 & 1 & -1 & -1 \\ 1 & -1 & 1 & -1 \\ 1 & -1 & -1 & 1 \end{pmatrix}, \quad \begin{matrix} j\delta = c+, c-, s+, s- \\ r\sigma = +\uparrow, +\downarrow, -\uparrow, -\downarrow \end{matrix}. \quad (34)$$

The transformation coefficients $B_{j\delta q}$ and $D_{j\delta q}$ in the case of the three modes $j\delta = c-, s+, s-$ are given by

$$B_{j\delta q} = 1 \text{ and } D_{j\delta q} = 0 \quad (35)$$

and for $j\delta = c+$ we obtain

$$B_{j\delta q} = \frac{1}{2}\left(\sqrt{g_q} + \frac{1}{\sqrt{g_q}} \right), D_{j\delta q} = \frac{1}{2}\left(\sqrt{g_q} - \frac{1}{\sqrt{g_q}} \right), \quad (36)$$

with $g_q = \frac{\varepsilon_{0q}}{\varepsilon_{c+q}}$. Small corrections to (35) and (36) resulting from the terms $V_{f^+\,b\,f^+}$ and $V_{b\,f^+/b\,f^+}$ have been neglected.

The physical meaning of the fermionic contributions in (32), depending on the number counting operators, have already been discussed subsequently to equations (30) and (31) respectively.

An eigenbasis of $H_0 + V_{\rho\rho}$ is formed by the states

$$|\boldsymbol{N}, \boldsymbol{m}\rangle := \prod_{j\delta q} \frac{\left(a^\dagger_{j\delta q} \right)^{m_{j\delta q}}}{\sqrt{m_{j\delta q}!}} |\boldsymbol{N}, 0\rangle, \quad (37)$$

where $|\boldsymbol{N}, 0\rangle$ has no bosonic excitation. Remember that the fermionic configuration $\boldsymbol{N} = (N_{-\uparrow}, N_{-\downarrow}, N_{+\uparrow}, N_{+\downarrow})$ defines the number of electrons in each of the branches $(r\sigma)$. In the following we will use the states from (37) as basis to examine the effect of $V_{\mathrm{n}\rho\rho}$. For this purpose we evaluate in the next section the corresponding matrix elements using the bosonization identity for the 1D electron operators.

3.2 The matrix elements $\langle \boldsymbol{N}\boldsymbol{m} | V_{\mathrm{n}\rho\rho} | \boldsymbol{N}'\boldsymbol{m}' \rangle$

Generally, due to $V_{\mathrm{n}\rho\rho}$, the quantities $\boldsymbol{N}$ and $\boldsymbol{m}$ are not conserved. Especially, the terms with $S_r = b, u$ in (26) mix states with different $\boldsymbol{N}$. However, denoting

$$N_s := \sum_{r\sigma} \mathrm{sgn}(\sigma) N_{r\sigma},$$

$$N_c^- := \sum_{r\sigma} \mathrm{sgn}(r) N_{r\sigma}$$

and

$$N_s^- := \sum_{r\sigma} \mathrm{sgn}(r\sigma) N_{r\sigma}$$

we find that (N_c, N_s, N_c^- mod 4, N_s^- mod 4) is conserved, i.e., states differing in those quantities do not mix, such that the corresponding matrix elements of $V_{\mathrm{n}\rho\rho}$ are zero. Note that in contrast to the real spin $S_z = \frac{1}{2}N_s$, the pseudo spin $\tilde{S}_z = \frac{1}{2}N_c^-$ is not conserved in general.

We already know that all the processes $V_{S_r S_F S_\sigma}$ contained in $V_{\mathrm{n}\rho\rho}$ are effectively local interactions, i.e., of the form (21). Hence, in order to calculate the corresponding matrix elements $\langle \boldsymbol{N}\boldsymbol{m}\,|V_{S_r S_F S_\sigma}|\,\boldsymbol{N'}\boldsymbol{m'}\rangle$ we first derive an expression for

$$M_{[r][F][\sigma]}(\boldsymbol{N},\boldsymbol{m},\boldsymbol{N'},\boldsymbol{m'},x) := \left\langle \boldsymbol{N}\boldsymbol{m}\left|\psi^\dagger_{r_1\sigma F_1}(x)\psi^\dagger_{r_2\sigma' F_2}(x)\psi_{r_3\sigma' F_3}(x)\psi_{r_4\sigma F_4}(x)\right|\boldsymbol{N'}\boldsymbol{m'}\right\rangle. \quad (38)$$

For this purpose we express the operators $\psi_{r\sigma F}(x)$ in terms of the bosonic operators $b_{\sigma r\cdot q}$ and $b^\dagger_{\sigma r\cdot q}$, $q>0$, using the bosonization identity [17],

$$\psi_{r\sigma F}(x) = \eta_{r\sigma} K_{r\sigma F}(x) e^{i\phi^\dagger_{r\sigma F}(x)} e^{i\phi_{r\sigma F}(x)}. \quad (39)$$

The operator $\eta_{r\sigma}$ is the so called Klein factor, which annihilates an electron in the $(r\sigma)$ branch and thereby takes care of the right sign as required from the fermionic anticommutation relations, in detail,

$$\eta_{r\sigma}\,|\boldsymbol{N},\boldsymbol{m}\rangle = (-1)^{\sum_{l=1}^{(r\sigma)-1} N_l}\,|\boldsymbol{N}-\hat{e}_{r\sigma},\boldsymbol{m}\rangle\,, \quad (40)$$

where we use the convention $l = +\uparrow, +\downarrow, -\uparrow, -\downarrow = 1,2,3,4$. $K_{r\sigma F}(x)$ yields a phase factor depending on the number of electrons in $(r\sigma)$,

$$K_{r\sigma F}(x) = \frac{1}{\sqrt{2L}} e^{i\frac{\pi}{L}\mathrm{sgn}(F)(r\cdot\mathcal{N}_{r\sigma}+\Delta)x}. \quad (41)$$

Finally, we have the boson fields $i\phi_{r\sigma F}(x)$,

$$i\phi_{r\sigma F}(x) = \sum_{q>0} \frac{1}{\sqrt{n_q}} e^{i\mathrm{sgn}(rF)qx} b_{\sigma r\cdot q}. \quad (42)$$

In Appendix B we are going to demonstrate with the help of the bosonization identity (39), that the matrix elements from equation (38) factorize into a fermionic and a bosonic part,

$$M_{[r][F][\sigma]}(\boldsymbol{N},\boldsymbol{m},\boldsymbol{N'},\boldsymbol{m'},x) = M_{[r][F][\sigma]}(\boldsymbol{N},\boldsymbol{N'},x) M_{[r][F][\sigma]}(\boldsymbol{m},\boldsymbol{m'},x),$$

where the fermionic part is given by

$$M_{[l]}(\boldsymbol{N},\boldsymbol{N'},x) = \langle \boldsymbol{N}|\,K^\dagger_{l_1}(x)\eta^\dagger_{l_1}K^\dagger_{l_2}(x)\eta^\dagger_{l_2}K_{l_3}(x)\eta_{l_3}K_{l_4}(x)\eta_{l_4}\,|\boldsymbol{N'}\rangle \quad (43)$$

and the bosonic part reads

$$M_{[l]}(\boldsymbol{m},\boldsymbol{m'},x) = \langle \boldsymbol{m}|\,e^{-i\phi^\dagger_{l_1}(x)}e^{-i\phi_{l_1}(x)}e^{-i\phi^\dagger_{l_2}(x)}e^{-i\phi_{l_2}(x)} e^{i\phi^\dagger_{l_3}(x)}e^{i\phi_{l_3}(x)}e^{i\phi^\dagger_{l_4}(x)}e^{i\phi_{l_4}(x)}\,|\boldsymbol{m'}\rangle\,. \quad (44)$$

In order to improve readability we have replaced the indices $rF\sigma$ by a single index l. As we demonstrate in Appendix B, the explicit evaluation yields

$$M_{[r][F][\sigma]}(\boldsymbol{N},\boldsymbol{N'},x) = \frac{1}{(2L)^2}\delta_{\boldsymbol{N},\boldsymbol{N'}+\boldsymbol{E}_{[r][\sigma]}} T_{\boldsymbol{N}\boldsymbol{N'}[r][\sigma]} Q_{\boldsymbol{N}\boldsymbol{N'}[r][F]}(x), \quad (45)$$

where $\boldsymbol{E}_{[r][\sigma]} := \boldsymbol{e}_{r_1\sigma} + \boldsymbol{e}_{r_2\sigma'} - \boldsymbol{e}_{r_3\sigma'} - \boldsymbol{e}_{r_4\sigma}$. The Klein factors in (39) lead to the sign factor $T_{\boldsymbol{N}\boldsymbol{N'}[r][\sigma]}$ which is either $+1$ or -1 and $Q_{\boldsymbol{N}\boldsymbol{N'}[r][F]}(x)$ yields a phase depending on $\boldsymbol{N}$. Explicit expressions can be found in Appendix B, equations (65) to (68).

For the bosonic part of $M_{[r][F][\sigma]}(\boldsymbol{N},\boldsymbol{m},\boldsymbol{N'},\boldsymbol{m'},x)$ the calculation in Appendix B leads to

$$M_{[r][F][\sigma]}(\boldsymbol{m},\boldsymbol{m'},x) = C_{[r][F][\sigma]}(x) \times A_{S_{rF}}(x)\prod_{j\delta q} F(\tilde{\lambda}^{j\delta q}_{[r][F][\sigma]}(x), m_{j\delta q}, m'_{j\delta q}). \quad (46)$$

Here the function $F(\lambda,m,m')$ stems from the evaluation of matrix elements of the form $\left\langle m\left|e^{-\lambda^* a^\dagger}e^{\lambda a}\right|m'\right\rangle$, where the bosonic excitations $|m\rangle$ are created by the operators $a^\dagger$, i.e., $|m\rangle = \left(a^\dagger\right)^m/\sqrt{m!}\,|0\rangle$. For the explicit form of $F(\lambda,m,m')$, and the coefficients $\tilde{\lambda}^{j\delta q}_{[r][F][\sigma]}(x)$, see Appendix B. The function $C_{[r][F][\sigma]}(x)$ is conveniently considered in combination with $Q_{\boldsymbol{N}\boldsymbol{N'}[r][F]}(x)$, namely the product

$$\tilde{K}_{\boldsymbol{N}[r][F][\sigma]}(x) := Q_{\boldsymbol{N}\boldsymbol{N'}[r][F]}(x) C_{[r][F][\sigma]}(x)$$

can be reexpressed as

$$\tilde{K}_{\boldsymbol{N}[r][F][\sigma]}(x) = \tilde{Q}_{\boldsymbol{N}[r][F]}(x)\tilde{C}_{S_r S_F S_\sigma}(x), \quad (47)$$

where

$$\tilde{Q}_{\boldsymbol{N}[r][F]}(x) = \exp\left[-i\frac{\pi}{L}\left(\tilde{\sum_{j=1}^{4}}\mathrm{sgn}(r_jF_j)N_{r_j\sigma_j} + \sum_{j=3}^{4}\mathrm{sgn}(r_jF_j)\right)x\right]$$

Here $\tilde{\sum}_{l=1}^{4} a_l$ denotes the sum $a_1 + a_2 - a_3 - a_4$. For $\tilde{C}_{S_r S_F S_\sigma}(x)$ we obtain

$$\tilde{C}_{f^+bf^-}(x) = -\tilde{C}_{f^-bf}(x) = -\tilde{C}_{bf^-f^+}(x) = 1/4\sin^2\left(\frac{\pi}{L}x\right), \quad (48)$$

$$\tilde{C}_{ubf^+}(x) = -\tilde{C}_{uf^-f^+}(x) = 4\sin^2\left(\frac{\pi}{L}x\right) \quad (49)$$

and $\tilde{C}_{S_r S_F S_\sigma}(x) \equiv 1$ for the remaining processes of $V_{\mathrm{n}\rho\rho}$.

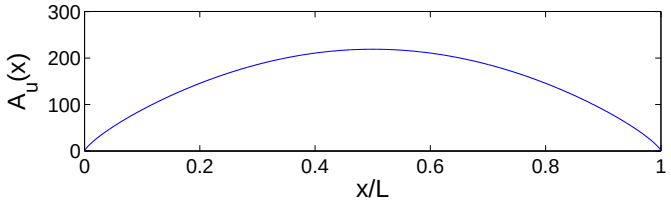

Fig. 4. $A_{S_{rF}=u}(x)$ as a function of x for a (6,6)-SWNT. Note the large magnitude of $A_{S_{rF}=u}(x)$ compared to $A_{S_{rF}\neq u}(x)\equiv 1$ for the processes only relevant away from half-filling!

The function $A_{S_{rF}}(x)$ is differing from 1 only for terms with $S_{rF}=u$, i.e., for the terms fulfilling condition (18) and which hence are relevant only near half-filling. The reason for this is that only for the $S_{rF}=u$ terms the coefficients $\tilde{\lambda}^{c+q}_{[r][F][\sigma]}(x)$ related to the charged c+mode are not vanishing. Hence $A_u(x)$ depends strongly on the energy dispersion of the c+ mode and therefore on the forward scattering part of the interaction, in detail

$$A_u(x)=\exp\left[2\sum_{q>0}\frac{1}{n_q}\left(1-\frac{\varepsilon_{0q}}{\varepsilon_{c+q}}\right)\sin^2(qx)\right].$$

Since for the repulsive Coulomb interaction $\varepsilon_{0q}/\varepsilon_{c+q}<1$ holds, we find $A_{S_{rF}=u}(x)\geq 1$. In Fig. 4 we show $A_{S_{rF}=u}(x)$ for a (6,6) SWNT. It is the large magnitude of $A_u(x)$, that poses problems for properly treating the situation at half-filling. Moreover we can expect that even for large diameter tubes, interaction processes with $S_{rF}=u$ can not be neglected near half-filling. Altogether, we get with equations (21), (45) and (46) for the single contributions to $V_{\mathrm{n}\rho\rho}$,

$$\begin{aligned}&\langle \boldsymbol{N}\boldsymbol{m}\,|V_{S_rS_FS_\sigma}|\,\boldsymbol{N}'\boldsymbol{m}'\rangle=\\&\times\frac{1}{4L}u^{S_rS_F}\sum_{\{[r]_{S_r},[F]_{S_F},[\sigma]_{S_\sigma}\}}\delta_{\boldsymbol{N},\boldsymbol{N}'+\boldsymbol{E}_{[r]\sigma\sigma'}}T_{\boldsymbol{N}S_rS_\sigma}\\&\times\int dx\,\tilde{K}_{\boldsymbol{N}[r][F]}(x)A_{S_{rF}}(x)\prod_{j\delta q}F(\tilde{\lambda}^{j\delta q}_{[r][F][\sigma]}(x),m_{j\delta q},m'_{j\delta q}).\end{aligned}\tag{50}$$

The evaluation of (50) causes no problems except for the $\boldsymbol{N}$ conserving processes with $(S_r,S_F,S_\sigma)=(f^+,b,f^-)$, (f^-,b,f), (b,f^-,f^+), since then we find $\tilde{K}_{\boldsymbol{N}[r][F][\sigma]}\sim 1/4\sin^2(\frac{\pi}{L}x)$, cf. equations (47) and (48), causing the integral in (50) to diverge for $\sum_{j\delta q}\left|m_{j\delta q}-m'_{j\delta q}\right|\leq 1$, such that the evaluation of the corresponding matrix elements needs special care in this case. The origin of this divergence lies in the fact, that if no bosonic excitations are present, the $\boldsymbol{N}$ conserving processes depend on the total number of electrons in the single branches (compare to the fermionic contributions to $H_0+V_{\rho\rho}$ in (32)). Since the bosonization approach requires the assumption of an infinitely deep Fermi sea [17] this leads, without the correct regularization, necessarily to divergencies. In Appendix C we show

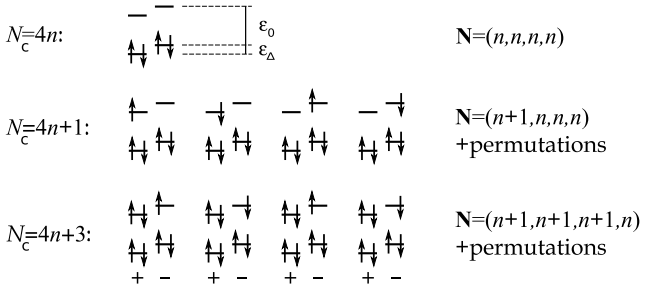

Fig. 5. The lowest lying eigenstates of $H_0+V_{\rho\rho}$ without bosonic excitations for the charge states $N_c=4n$, $N_c=4n+1$ and $N_c=4n+3$. On the right side the fermionic configurations are given. We use the convention $\boldsymbol{N}=(N_{+\uparrow},N_{+\downarrow},N_{-\uparrow},N_{-\downarrow})$.

exemplarily the proper calculation for $\langle \boldsymbol{N}\boldsymbol{m}\,|V_{f^+\,b\,f^-}|\,\boldsymbol{N}\boldsymbol{m}'\rangle$. We here give the regularized result for $\boldsymbol{m}=\boldsymbol{m}'$, since it is of special importance for the discussion of the ground state spectra away from half-filling,

$$\begin{aligned}\langle \boldsymbol{N}\boldsymbol{m}\,|V_{f^+\,b\,f^-}|\,\boldsymbol{N}\boldsymbol{m}\rangle&=u^+\sum_r\min(N_{r\uparrow},N_{r\downarrow})\\&+\frac{1}{4L}u^+\sum_{\{[r]_{f^+},[F]_b,[\sigma]_{f^-}\}}\int dx\tilde{K}_{\boldsymbol{N}[r][F]}(x)\\&\times\left(\prod_{j\delta q}F(\lambda^{j\delta q}_{[r][F][\sigma]}(x),m_{j\delta q},m_{j\delta q})-1\right).\end{aligned}\tag{51}$$

4 The SWNT spectrum

In Section 3.1 we wave diagonalized $H_0+V_{\rho\rho}$ and in Section 3.2 we have determined the matrix elements of $V_{\mathrm{n}\rho\rho}$ in the eigenbasis of $H_0+V_{\rho\rho}$. Away from half-filling the magnitude of $V_{\mathrm{n}\rho\rho}$ is only small compared to $H_0+V_{\rho\rho}$ and therefore we can easily analyze the effect of the non-density-density interaction $V_{\mathrm{n}\rho\rho}$ on the SWNT spectrum by representing the total Hamiltonian $H_0+V_{\rho\rho}+V_{\mathrm{n}\rho\rho}$ in a truncated eigenbasis of $H_0+V_{\rho\rho}$.

4.1 The low energy spectrum away from half-filling

We start with the examination of the ground and low energy states. As basis we use the lowest lying eigenstates of $H_0+V_{\rho\rho}$ without bosonic excitations with a given number of electrons N_c.

4.1.1 $N_c=4n$, $N_c=4n+1$, $N_c=4n+3$

First we consider the charge states $N_c=4n$, $N_c=4n+1$ and $N_c=4n+3$. In that case the lowest lying eigenstates of $H_0+V_{\rho\rho}$, shown in Fig. 5, which are of the form $|\boldsymbol{N},0\rangle$ and therefore uniquely characterized by $\boldsymbol{N}$, do not mix via $V_{\mathrm{n}\rho\rho}$. That means that the only correction from $V_{\mathrm{n}\rho\rho}$ to $H_0+V_{\rho\rho}$ stems from the $\boldsymbol{N}$ conserving process

$V_{f^+\,b\,f^-}$. For states without bosonic excitations, equation (51) yields, because of $F(\lambda,0,0)=1$,

$$\langle \boldsymbol{N},0\,|V_{\mathrm{n}\rho\rho}|\,\boldsymbol{N},0\rangle = \left\langle \boldsymbol{N},0\,\middle|V_{f^+\,b\,f^-}\middle|\,\boldsymbol{N},0\right\rangle = u^+\sum_r \min(N_{r\uparrow},N_{r\downarrow}). \quad (52)$$

Hence here $V_{\mathrm{n}\rho\rho}$ yields an energy penalty for occupying the same branch r. This effect has already been found in the meanfield theory of Oreg et al. [10]. The parameter δU there corresponds to our constant u^+. The energies of the lowest lying states for $N_c=4n$, $N_c=4n+1$ and $N_c=4n+3$ only depend on $\boldsymbol{N}$. In detail we find with (32) and (52),

$$E_{\boldsymbol{N}} = \frac{1}{2}E_c\mathcal{N}_c^2 + u^+\sum_r \min(N_{r\uparrow},N_{r\downarrow}) + \frac{1}{2}\sum_{r\sigma}\mathcal{N}_{r\sigma}\left[-\frac{J}{2}\mathcal{N}_{-r\sigma} + \left(\varepsilon_0-u^+\right)\mathcal{N}_{r\sigma} + r\varepsilon_\Delta\right]. \quad (53)$$

From (53) it follows that for the states depicted in Fig. 5 the interaction dependent part of $E_{\boldsymbol{N}}$ is the same for all fermionic configurations $\boldsymbol{N}$ corresponding to a given charge state N_c. Hence the interaction leads merely to a common shift of the lowest lying energy levels for fixed N_c.

4.1.2 $N_c = 4n+2$

Of special interest is the ground state structure of the $N_c=4n+2$ charge state, since here the lowest lying six eigenstates of $H_0+V_{\rho\rho}$ without bosonic excitations, denoted $|\boldsymbol{N},0\rangle$ with $\boldsymbol{N}=(n+1,n+1,n,n)+$permutations, mix via $V_{\mathrm{n}\rho\rho}$, leading to a $S=1$ triplet state and to three nondegenerate states with spin 0. For $\varepsilon_\Delta\approx 0$ (the meaning of ≈ 0 will become clear in the following) the triplet is the ground state. In the following we are going to denote $|(n+1,n+1,n,n),0\rangle$ by $|\uparrow\downarrow,-\rangle$, $|(n+1,n,n,n+1),0\rangle$ by $|\uparrow,\downarrow\rangle$ and analogously for the remaining four states. Ignoring interactions, the six considered states are degenerate for $\varepsilon_\Delta=0$. As we can conclude from (32) the degeneracy of the six considered states is already lifted if including only the density-density interaction $V_{\rho\rho}$, since then the energy of the spin 1 states $|\uparrow,\uparrow\rangle$ and $|\downarrow,\downarrow\rangle$ is lowered by

$$J/2 := u_f^\Delta + u_b^\Delta \quad (54)$$

relatively to the other ground states. Let us now consider the effects of $V_{\mathrm{n}\rho\rho}$. The diagonal matrix elements $\langle \boldsymbol{N},0\,|V_{\mathrm{n}\rho\rho}|\,\boldsymbol{N},0\rangle$ are again determined by equation (52), leading to a relative energy penalty for the states $|\uparrow\downarrow,-\rangle$ and $|-,\uparrow\downarrow\rangle$. Mixing occurs between the states $|\uparrow,\downarrow\rangle$ and $|\downarrow,\uparrow\rangle$ via $V_{b\,f^+\,f^-}$ and $V_{b\,b\,f^-}$ and between $|\uparrow\downarrow,-\rangle$ and $|-,\uparrow\downarrow\rangle$ via $V_{u\,f^-\,f^-}$ and $V_{u\,b\,f^-}$. With equation (50) we find

$$\langle\uparrow,\downarrow|V_{\mathrm{n}\rho\rho}|\downarrow,\uparrow\rangle = -\frac{J}{2} = -\langle\uparrow\downarrow,-|V_{\mathrm{n}\rho\rho}|-,\uparrow\downarrow\rangle.$$

In total, the SWNT Hamiltonian $H=H_0+V_{\rho\rho}+V_{\mathrm{n}\rho\rho}$ restricted to the basis spanned by the six states $|\uparrow,\uparrow\rangle$, $|\downarrow,\downarrow\rangle$, $|\uparrow,\downarrow\rangle$, $|\downarrow,\uparrow\rangle$, $|\uparrow\downarrow,-\rangle$ and $|-,\uparrow\downarrow\rangle$ is represented by the matrix,

$$H = E_{0,4n+2} + \begin{pmatrix} -\frac{J}{2} & & & & & 0 \\ & -\frac{J}{2} & & & & \\ & & 0 & -\frac{J}{2} & & \\ & & -\frac{J}{2} & 0 & & \\ & & & & u^+-\varepsilon_\Delta & \frac{J}{2} \\ 0 & & & & \frac{J}{2} & u^++\varepsilon_\Delta \end{pmatrix}, \quad (55)$$

where $E_{0,4n+2}=\frac{1}{2}E_cN_c^2+(2n^2+2n+1)(\varepsilon_0-u^+)-J(n^2+n)+2u^+n$. Diagonalizing the matrix in (55), we find that its eigenstates are given by the spin 1 triplet

$$|\uparrow,\uparrow\rangle, |\uparrow,\uparrow\rangle, 1/\sqrt{2}\,(|\uparrow,\downarrow\rangle+|\downarrow,\uparrow\rangle),$$

the spin 0 singlet

$$1/\sqrt{2}\,(|\uparrow,\downarrow\rangle-|\downarrow,\uparrow\rangle)$$

and the two states

$$\frac{1}{\sqrt{c_{1/2}^2+1}}\left(c_{1/2}\,|\uparrow\downarrow,-\rangle \pm |-,\uparrow\downarrow\rangle\right),$$

where the coefficients $c_{1/2}$ are given by

$$c_{1/2} = \frac{\sqrt{\varepsilon_\Delta^2+(J/2)^2}\mp\varepsilon_\Delta}{J/2}.$$

Relatively to $E_{0,4n+2}$, the corresponding eigenenergies are $-J/2$ for the triplet states, $J/2$ for the singlet state and $u^+\pm\sqrt{\varepsilon_\Delta^2+(J/2)^2}$ for the remaining two states. Thus under the condition

$$J/2 > \sqrt{\varepsilon_\Delta^2+(J/2)^2}-u^+,$$

i.e., for a small band mismatch $\varepsilon_\Delta \lesssim J/2$ the ground state is degenerate and formed by the spin 1 triplet, otherwise by $\frac{1}{\sqrt{c_2^2+1}}(c_2\,|\uparrow\downarrow,-\rangle+|-,\uparrow\downarrow\rangle)$. The ground state spectra for the two cases $\varepsilon_\Delta=0$ and $\varepsilon_\Delta\gg J/2$ are shown in Fig. 6 for a (6,6) armchair SWNT (corresponding to a diameter of 0.8 nm). Assuming a dielectric constant of $\varepsilon=1.4$ [1], the calculation of the coupling parameters according to Appendix A yields values of $J=2(u_f^\Delta+u_b^\Delta)=0.09\varepsilon_0$ and $u^+\approx 0.03\varepsilon_0$ which agree well with the experiments [7,9], where nanotubes with $\varepsilon_\Delta\gg J/2$ were considered. To our knowledge, experiments in the regime $\varepsilon_\Delta\lesssim J/2$ demonstrating exchange effects have not been carried out so far, such that a validation of our predictions for this case, namely the existence of the ground state spin 1 triplet and the mixing of the states $|\uparrow\downarrow,-\rangle$ and $|-,\uparrow\downarrow\rangle$ is still missing. The latter effect could be of relevance for the understanding of the so called singlet-triplet Kondo effect [19] in SWNTs.

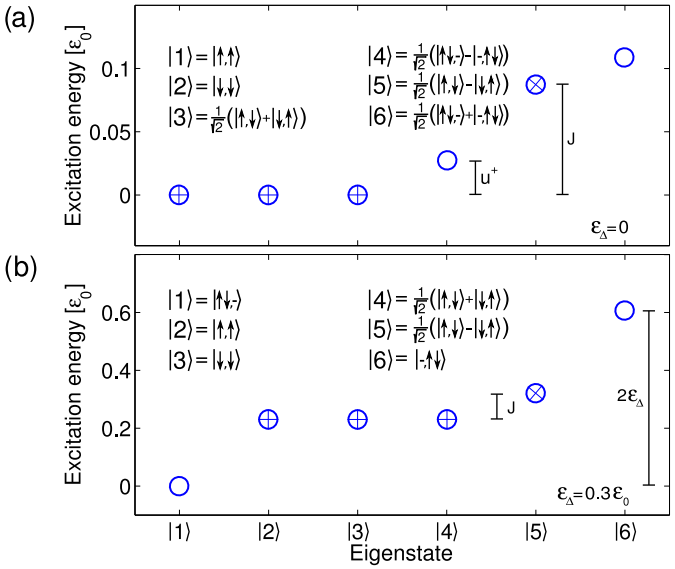

Fig. 6. Low energy spectrum of a $(6,6)$ SWNT for the charge state $N_c = 4n+2$. (a) In the case $\varepsilon_\Delta = 0$ the ground state is formed by the spin 1 triplet ($\rightarrow \oplus$) and the states $|\uparrow\downarrow,-\rangle$ and $|-,\uparrow\downarrow\rangle$ mix ($\rightarrow \bigcirc$ states). (b) For $\varepsilon_\Delta \gg J/2$ the ground state is given by the spin 0 state $|\uparrow\downarrow,-\rangle$.
The spin 0 singlet state $1/\sqrt{2}\,(|\uparrow,\downarrow\rangle - |\downarrow,\uparrow\rangle)$ is indicated by $\otimes$. The coupling parameters are $J = 0.09\varepsilon_0$ and $u^+ \approx 0.03\varepsilon_0$.

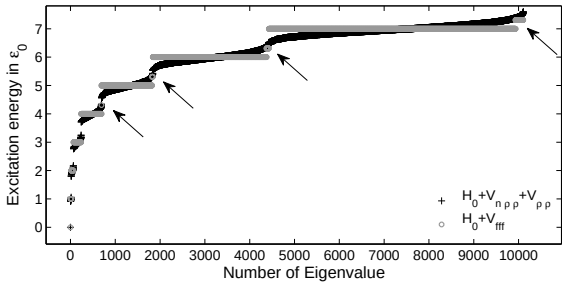

Fig. 7. The excitation spectrum for a (6,6) SWNT occupied by $N_c = 4n$ electrons. In grey we show the spectrum as obtained by diagonalizing the Hamiltonian of the standard theory $H_{st} = H_0 + V_{f\,f\,f}$ and in black for the full Hamiltonian $H = H_0 + V_{\rho\rho} + V_{\mathrm{n}\rho\rho}$. A band mismatch $\varepsilon_\Delta = 0$ is assumed. The energy of the lowest $c+$ excitation is $4.3\varepsilon_0$. All other interaction parameters are as in Fig. 6. Arrows indicate eigenenergies of the "standard" Hamiltonian $H_{st} = H_0 + V_{f\,f\,f}$ involving excitations of the $c+$ mode.

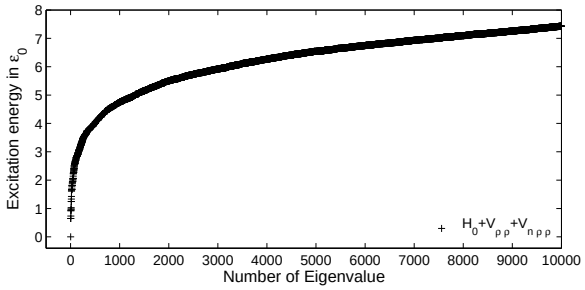

Fig. 8. The excitation spectrum for a (6,6) SWNT obtained by diagonalizing the full Hamiltonian $H = H_0 + V_{\rho\rho} + V_{\mathrm{n}\rho\rho}$ for $N_c = 4m$ and $\varepsilon_\Delta = 0.3\varepsilon_0$. The spectrum becomes quasicontinuous at relatively small energies. Shown are the lowest 10000 eigenenergies.

It should be stressed that all exchange effects, leading amongst others to the spin 1 triplet as ground state, result from $S_r \neq f$ interaction processes. In the work of Mattis and Lieb [11] however, there is no such additional pseudo spin degree of freedom. Hence we suspect that this is the reason why their theorem can not be applied in our situation.

4.2 Excitation spectra away from half-filling

Until now our discussion of the energy spectra was based on states $|\boldsymbol{N},0\rangle$ without bosonic excitations and so far the effect of $V_{\mathrm{n}\rho\rho}$ on the spectrum could have even been treated without using bosonization. But for the determination of the excitation spectrum of H we do need the general expression for the matrix elements of $V_{\mathrm{n}\rho\rho}$ between the eigenstates of $H_0 + V_{\rho\rho}$ as given by (50). For the actual calculation we truncate the eigenbasis of $H_0 + V_{\rho\rho}$ for a fixed charge state N_c at a certain excitation energy and represent H in this shortened basis. After the diagonalization we find to a good approximation the correct eigenstates and eigenenergies of H. For the results shown in Figs. 7 to 10 we have checked that convergence has been reached, i.e., the extention of the considered basis states does not lead to a significant change of the spectrum.

Exemplarily we present the results for the charge state $N = 4n$. Similar excitation spectra are found for the other charge states. In Fig. 7 we show for comparison and in order to demonstrate the effect of the non forward scattering processes the findings for the "standard" theory, i.e., the spectrum of $H_{st} = H_0 + V_{f\,f\,f}$ as well as the spectrum of the full Hamiltonian $H = H_0 + V_{\rho\rho} + V_{\mathrm{n}\rho\rho}$ for a $(6,6)$ armchair nanotube. Thereby a nonvanishing band mismatch $\varepsilon_\Delta = 0$ is assumed. Striking is the partial breaking of the huge degeneracies of the "standard" spectrum. Note also the lifting of the spin-charge separation when including the non forward scattering processes. To illustrate this point we have indicated eigenenergies of H_{st} including $c+$ excitations by arrows in Fig. 7.

At higher energies a quasi continuum forms in the case of the full Hamiltonian H, a feature becoming especially apparent for a finite band mismatch. In Fig. 8 the spectra of the full Hamiltonian H is shown for $\varepsilon_\Delta = 0.3\varepsilon_0$.

As we have already discussed, the importance of non forward scattering terms should decrease with increasing tube diameter. And indeed the excitation spectrum of the full Hamiltonian for a $(20,20)$ SWNT resembles much more the result of the "standard" theory than it is the case for a $(6,6)$ SWNT as it can be seen from Fig. 9.

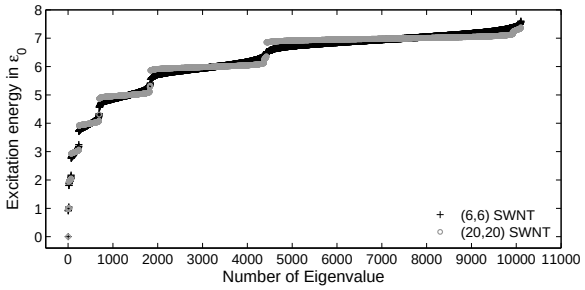

Fig. 9. The excitation spectrum for a (6,6) SWNT (black) compared to the spectrum of a (20,20) SWNT (grey). The effects of the non forward scattering processes are by far less pronounced in the latter case. $N_c = 4m$ and $\varepsilon_\Delta = 0$.

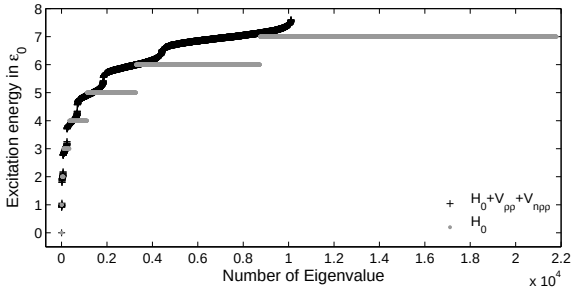

Fig. 10. The excitation spectrum for a (6,6) SWNT obtained by diagonalizing the Hamiltonian of the noninteracting system H_0 (grey) and the full Hamiltonian $H = H_0 + V_{\rho\rho} + V_{\mathrm{n}\rho\rho}$ (black).

It is also interesting to regard the effect of the total interaction $V_{\rho\rho} + V_{\mathrm{n}\rho\rho}$ on the nanotube spectrum. For this purpose, in Fig. 10 the spectrum of H_0 describing the noninteracting system is compared to the spectrum of the full Hamiltonian H, again for a $(6,6)$ SWNT with vanishing band mismatch. Of special significance is the strong reduction of the number of eigenstates below a certain energy if the interaction is "switched on". This can be mainly traced back to V_{fff} which leads to the formation of the bosonic $c+$ excitations with considerably enlarged energies. Concerning the transport properties of SWNTs the reduction of relevant states plays an important role for the occurrence of the power law dependence of various transport quantities in the case of infinitely long tubes but also for the appearance of negative differential conductance in highly asymmetric SWNT quantum dots as described in [6].

4.3 Comparison to the mean field results

We shortly want to compare the results of the meanfield theory by Oreg et al. [10] and our approach. Concerning the groundstate structure, differences between the two works arise for the $N_c = 4m + 2$ charge state. In this situation the meanfield Hamiltonian can essentially be recovered by setting all off-diagonal elements in (55) to zero. Therefore in [10] the degenerate triplet state can not be predicted but twofold degeneracies of the states $|\uparrow,\uparrow\rangle$, $|\downarrow,\downarrow\rangle$ and of $|\uparrow,\downarrow\rangle$, $|\downarrow,\uparrow\rangle$ respectively are found. Moreover contrary to our theory in [10] no mixing of the states $|\uparrow\downarrow,-\rangle$ and $|-,\uparrow\downarrow\rangle$ can occur for $\varepsilon_\Delta \lesssim J/2$, an important point regarding the singlet-triplet Kondo effect [19].

Moreover also the excitation spectrum shows considerable differences in both approaches, since the meanfield approach misses the formation of the collective electronic excitations as the $c+$ mode, with its dispersion relation strongly renormalized by the forward scattering part of the Coulomb interaction.

4.4 Near half-filling

As we have already seen in Section 3.2, at half-filling non-density-density interaction processes become relevant which yield tremendously large matrix elements in the eigenbasis of $H_0 + V_{\rho\rho}$, as a consequence of the function $A_u(x)$ shown in Fig. 4. Therefore our truncation scheme for diagonalizing the total Hamiltonian $V_{n\rho\rho}$ does not give reliable results at half-filling. Investigation of the half-filling case is beyond the scope of this work.

5 Conclusions

In summary, we have derived the low energy Hamiltonian for metallic finite size SWNTs including all relevant interaction terms, especially the short ranged processes whose coupling strength scales inversely proportional to the SWNT size. The Hamiltonian of the noninteracting system, H_0, together with the density-density part of the interaction, $V_{\rho\rho}$, could be diagonalized by bosonization and Bogoliubov transformation. Considering only the situation away from half-filling, we obtained the spectrum of the total SWNT Hamiltonian by exploiting the small magnitude of the non-density-density contribution $V_{\mathrm{n}\rho\rho}$ to the interaction: we have calculated the matrix elements of $V_{\mathrm{n}\rho\rho}$ in a truncated eigenbasis of $H_0 + V_{\rho\rho}$ and diagonalized the resulting matrix to obtain the SWNT spectrum and the corresponding eigenstates.

Of special interest, concerning the ground state spectra, is the formation of a spin 1 triplet for the charge state $N_c = 4m + 2$, whose existence has clearly been proven in the experiments of Moriyama et al. [9]. In the case of a band mismatch ε_Δ that is small compared to the exchange energy J, the spin 1 triplet is the ground state of the system. This finding is interesting since according to a theorem by Lieb and Mattis [11], only ground states with spin 0 or 1/2 are allowed for a 1D Hubbard model with next-neighbour hopping and no orbital degeneracies. Since our SWNT Hamiltonian includes an orbital degree of freedom we conclude that scattering processes with respect to this degree of freedom are the reason for the finding of a spin 1 ground state. Additionally we predict for $\varepsilon_\Delta \lesssim J/2$, the

mixing of the states $|\uparrow\downarrow,-\rangle$ and $|-,\uparrow\downarrow\rangle$ with an accompanying energy splitting. The degree of mixing between $|\uparrow\downarrow,-\rangle$ and $|-,\uparrow\downarrow\rangle$ is of importance for the singlet-triplet Kondo effect, as discussed in [19]. An experimental confirmation of our findings in the case $\varepsilon_\Delta \lesssim J/2$ is still missing, but well within reach.

With regard to the excitation spectrum, the different bosonic modes are mixed by the non-density-density interaction processes $V_{\mathrm{n}\rho\rho}$. Therefore the spin-charge separation is lifted. Moreover we find that the huge degeneracies which are obtained by the "standard" theory that retains only forward scattering processes are partially broken. This leads to a more and more continuous energy spectrum for higher energies.

A Modelling the interaction potential

In this Appendix we show how we determine the values of the effective 1D potentials $U_{[F]}^{intra/inter}$ and of the coupling constants $u^{S_r\,S_F}$. We start with equation (12) from section 2.2,

$$U_{[F]}^{intra/inter}(x,x') = L^2 \int\int d^2r_\perp d^2r'_\perp \times \varphi^*_{pF_1}(\boldsymbol{r})\varphi^*_{\pm pF_2}(\boldsymbol{r}')\varphi_{\pm pF_3}(\boldsymbol{r}')\varphi_{pF_4}(\boldsymbol{r})U(\boldsymbol{r}-\boldsymbol{r}'). \quad (56)$$

Using equation (4) in order to reexpress the Bloch waves $\varphi_{pF}(\boldsymbol{r})$ in terms of p_z orbitals, we obtain,

$$U_{[F]}^{intra/inter}(x,x') = \frac{L^2}{N_L^2}\int\int d^2r_\perp d^2r'_\perp \times U(\boldsymbol{r}-\boldsymbol{r}')\sum_{\boldsymbol{R},\boldsymbol{R}'} e^{-i(F_1-F_4)R_x - i(F_2-F_3)R'_x} \times |\chi(\boldsymbol{r}-\boldsymbol{R}-\boldsymbol{\tau}_p)|^2\,|\chi(\boldsymbol{r}'-\boldsymbol{R}'-\boldsymbol{\tau}_{\pm p})|^2. \quad (57)$$

Instead of a fourfold sum over the lattice sites only the double sum $\sum_{\boldsymbol{R},\boldsymbol{R}'}$ remains, since the overlap of different p_z orbitals can be neglected. To proceed we use once more that the spatial extention of the p_z orbitals is small compared to all other appearing length scales and therefore replace $|\chi(\boldsymbol{r}-\boldsymbol{R}-\boldsymbol{\tau}_p)|^2$ by the delta function $\delta(\boldsymbol{r}-\boldsymbol{R}-\boldsymbol{\tau}_p)$. In order to take into account the error induced thereby at small distances $x \approx x'$, we replace the Coulomb potential by the Ohno potential introduced by equation (8). It interpolates between U_0, the interaction energy between two p_z electrons in the same orbital and $\frac{e^2}{4\pi\epsilon_0\epsilon|\boldsymbol{r}-\boldsymbol{r}\,'|}$ for $|\boldsymbol{r}-\boldsymbol{r}\,'| \gg 0$. Performing the integration in (57), we obtain,

$$U_{[F]}^{intra/inter}(x,x') = \frac{L^2}{N_L^2}\sum_{\boldsymbol{R},\boldsymbol{R}'}\delta(x-R_x)\delta(x'-R'_x) \times e^{-i(F_1-F_4)R_x - i(F_2-F_3)R'_x}U(\boldsymbol{R}-\boldsymbol{R}'+\boldsymbol{\tau}_p-\boldsymbol{\tau}_{\pm p}). \quad (58)$$

Now we can easily calculate the values of the coupling constants $u^{S_r\,S_F}$ for the local interactions, given by (20),

$$u^{S_r\,S_F} = 1/(2L^2)\int\int dx\,dx' U_{[r]_{S_r}[F]_{S_F}}(x,x').$$

Using (58) together with equation (11),

$$U_{[r][F]}(x,x') = \frac{1}{4}\left[U_{[F]}^{intra}(x,x')(1+r_1r_2r_3r_4) + U_{[F]}^{inter}(x,x')(r_2r_3+r_1r_4)\right], \quad (59)$$

we arrive at

$$u^{f\,b} =: u^+ = \frac{1}{4N_L^2}\sum_{\boldsymbol{R},\boldsymbol{R}'} e^{-i2K_0(R_x-R'_x)} \times \left[U(\boldsymbol{R}-\boldsymbol{R}')+U(\boldsymbol{R}-\boldsymbol{R}'+\boldsymbol{\tau}_p-\boldsymbol{\tau}_{-p})\right], \quad (60)$$

$$u^{b/u\,f} =: u_f^\Delta = \frac{1}{4N_L^2}\sum_{\boldsymbol{R},\boldsymbol{R}'}\left[U(\boldsymbol{R}-\boldsymbol{R}')-U(\boldsymbol{R}-\boldsymbol{R}'+\boldsymbol{\tau}_p-\boldsymbol{\tau}_{-p})\right] \quad (61)$$

and

$$u^{b/u\,f} =: u_b^\Delta = \frac{1}{4N_L^2}\sum_{\boldsymbol{R},\boldsymbol{R}'} e^{-i2K_0(R_x-R'_x)} \times \left[U(\boldsymbol{R}-\boldsymbol{R}')-U(\boldsymbol{R}-\boldsymbol{R}'+\boldsymbol{\tau}_p-\boldsymbol{\tau}_{-p})\right]. \quad (62)$$

Since in the summations in (60), (61) and (62) only terms with $\boldsymbol{R} \approx \boldsymbol{R}'$ contribute, the number of relevant summands scales like the number of lattice sites N_L. Due to the prefactor $1/N_L^2$, u^+ and $u_{f/b}^\Delta$ in total scale like $1/N_L$. Numerical evaluation of the previous three equations leads to the values given in table 1.

B Calculation of the matrix elements $M_{[r][F][\sigma]}(\boldsymbol{N},\boldsymbol{m},\boldsymbol{N}',\boldsymbol{m}',x)$

Using the bosonization identity (39),

$$\psi_{r\sigma F}(x) = \eta_{r\sigma}K_{r\sigma F}(x)e^{i\phi^\dagger_{r\sigma F}(x)}e^{i\phi_{r\sigma F}(x)},$$

we can separate $M_{[r][F][\sigma]}(\boldsymbol{N},\boldsymbol{m},\boldsymbol{N}',\boldsymbol{m}',x)$ from equation (38) into a bosonic and a fermionic part,

$$M_{[r][F][\sigma]}(\boldsymbol{N},\boldsymbol{m},\boldsymbol{N}',\boldsymbol{m}',x) = M_{[r][F][\sigma]}(\boldsymbol{N},\boldsymbol{N}',x)M_{[r][F][\sigma]}(\boldsymbol{m},\boldsymbol{m}',x),$$

where

$$M_{[l]}(\boldsymbol{N},\boldsymbol{N}',x) = \langle\boldsymbol{N}|\,K^\dagger_{l_1}(x)\eta^\dagger_{l_1}K^\dagger_{l_2}(x)\eta^\dagger_{l_2}K_{l_3}(x)\eta_{l_3}K_{l_4}(x)\eta_{l_4}\,|\boldsymbol{N}'\rangle \quad (63)$$

and

$$M_{[l]}(\boldsymbol{m},\boldsymbol{m}',x) = \langle\boldsymbol{m}|\,e^{-i\phi^\dagger_{l_1}(x)}e^{-i\phi_{l_1}(x)}e^{-i\phi^\dagger_{l_2}(x)}e^{-i\phi_{l_2}(x)} e^{i\phi^\dagger_{l_3}(x)}e^{i\phi_{l_3}(x)}e^{i\phi^\dagger_{l_4}(x)}e^{i\phi_{l_4}(x)}\,|\boldsymbol{m}'\rangle. \quad (64)$$

Improving readability, we have summarized the indices $rF\sigma$ by a single index l.

B.1 The Fermionic part of $M_{[r][F][\sigma]}(\boldsymbol{N},\boldsymbol{m},\boldsymbol{N}',\boldsymbol{m}',x)$

First we consider the contribution $M_{[l]}(\boldsymbol{N},\boldsymbol{N}',x)$ depending on the fermionic configurations $\boldsymbol{N}$ and $\boldsymbol{N}'$. Using relation (40) for the Klein factors $\eta_{r\sigma}$ and the definition of the phase factor $K_{r\sigma F}(x)$, equation (41), we obtain

$$M_{[r][F][\sigma]}(\boldsymbol{N},\boldsymbol{N}',x) = \frac{1}{(2L)^2}\delta_{\boldsymbol{N},\boldsymbol{N}'+\boldsymbol{E}_{[r][\sigma]}} T_{\boldsymbol{N}\boldsymbol{N}'[r][\sigma]} Q_{\boldsymbol{N}\boldsymbol{N}'[r][F]}(x),$$

where $\boldsymbol{E}_{[r][\sigma]} := \boldsymbol{e}_{r_1\sigma} + \boldsymbol{e}_{r_2\sigma'} - \boldsymbol{e}_{r_3\sigma'} - \boldsymbol{e}_{r_4\sigma}$. Furthermore $T_{\boldsymbol{N}\boldsymbol{N}'[r][\sigma]}$ is given by

$$T_{\boldsymbol{N}\boldsymbol{N}'[r][\sigma]} = (-1)^{\sum_{j_4=1}^{(r_4\sigma_4)-1}(\boldsymbol{N}')_{j_4}+\sum_{j_3=1}^{(r_3\sigma_3)-1}(\boldsymbol{N}'-\boldsymbol{e}_{r_4\sigma_4})_{j_3}} \times (-1)^{\sum_{j_2=1}^{(r_2\sigma_2)-1}(\boldsymbol{N}-\boldsymbol{e}_{r_1\sigma_1})_{j_2}+\sum_{j_1=1}^{(r_1\sigma_1)-1}(\boldsymbol{N})_{j_1}}. \quad (65)$$

Here we use the convention $j = +\uparrow, +\downarrow, -\uparrow, -\downarrow = 1,2,3,4$. It turns out that $T_{\boldsymbol{N}\boldsymbol{N}'[r][\sigma]}$ only depends on the scattering types S_r and S_σ. Explicitly with $T_{\boldsymbol{N}'S_rS_\sigma} := T_{\boldsymbol{N}\boldsymbol{N}'[r]_{S_r}[\sigma]_{S_\sigma}}$,

$$T_{\boldsymbol{N}'uf^-} = -(-1)^{3N'_{R\uparrow}+2N'_{R\downarrow}+N'_{L\uparrow}}, \quad (66)$$

$$T_{\boldsymbol{N}'bf^-} = (-1)^{3N'_{R\uparrow}+2N'_{R\downarrow}+N'_{L\uparrow}} \quad (67)$$

and $T_{\boldsymbol{N}'S_rS_\sigma} = 1$ for all other (S_r,S_σ). Finally the function $Q_{\boldsymbol{N}\boldsymbol{N}'[r][F]}(x)$ yields a phase and is given by

$$Q_{\boldsymbol{N}\boldsymbol{N}'[r][F]}(x) = \exp\left\{ i\frac{\pi}{L}\left[\mathrm{sgn}(r_4F_4)(\boldsymbol{N}')_{l_4} + \mathrm{sgn}(r_3F_3)(\boldsymbol{N}'-\hat{e}_{l_4})_{l_3} - \mathrm{sgn}(r_2F_2)(\boldsymbol{N}-\hat{e}_{l_1})_{l_2} - \mathrm{sgn}(r_1F_1)(\boldsymbol{N})_{l_1}\right] x\right\}. \quad (68)$$

B.2 The bosonic part of $M_{[r][F][\sigma]}(\boldsymbol{N},\boldsymbol{m},\boldsymbol{N}',\boldsymbol{m}',x)$

The calculation of the bosonic part $M_{[r][F][\sigma]}(\boldsymbol{m},\boldsymbol{m}',x)$ is based on expressing the fields $i\phi_{r\sigma F}(x)$ in equation (64) in terms of the bosonic operators $a_{j\delta q}$, $a^\dagger_{j\delta q}$ and subsequent normal ordering, i.e., commuting all annihilation operators $a_{j\delta q}$ to the right side and all creation operators $a^\dagger_{j\delta q}$ to the left side. In a first step we use the relation

$$e^{i\phi_l(x)}e^{i\phi_l^\dagger(x)} = e^{i\phi_l^\dagger(x)}e^{i\phi_l(x)}e^{[i\phi_l(x),i\phi_l^\dagger(x)]},$$

following from the Baker-Hausdorff formula [17],

$$e^Ae^B = e^{A+B}e^{\frac{1}{2}[A,B]},\ [A,B]\in\mathbb{C},$$

to obtain from (64),

$$M_{[l]}(\boldsymbol{m},\boldsymbol{m}',x) = C_{[l]}(x) \times \left\langle \boldsymbol{m}\left| e^{-i\tilde{\sum}_{n=1}^4\phi^\dagger_{l_n}(x)}e^{-i\tilde{\sum}_{n=1}^4\phi_{l_n}(x)}\right|\boldsymbol{m}'\right\rangle, \quad (69)$$

where $\tilde{\sum}_{l=1}^4\phi_{l_n}$ denotes the sum $\phi_{l_1}+\phi_{l_2}-\phi_{l_3}-\phi_{l_4}$ and

$$C_{[l]}(x) = e^{[i\phi_{l_3}(x),i\phi^\dagger_{l_4}(x)]}e^{[-i\phi_{l_2}(x),i\phi^\dagger_{l_3}(x)+i\phi^\dagger_{l_4}(x)]} \times e^{[-i\phi_{l_1}(x),-i\phi^\dagger_{l_2}(x)+i\phi^\dagger_{l_3}(x)+i\phi^\dagger_{l_4}(x)]}.$$

Applying the Baker-Hausdorff formula once more, we obtain

$$e^{-i\tilde{\sum}_{n=1}^4\phi^\dagger_{l_n}(x)}e^{-i\tilde{\sum}_{n=1}^4\phi_{l_n}(x)} = e^{-i\tilde{\sum}_{n=1}^4\left(\phi_{l_n}(x)+\phi^\dagger_{l_n}(x)\right)}e^{\frac{1}{2}\left[i\tilde{\sum}_{n=1}^4\phi^\dagger_{l_n}(x),i\tilde{\sum}_{n'=1}^4\phi_{l_{n'}}(x)\right]}.$$

Using the definition of the ϕ-fields, equation (42), together with the transformation between the operators $b_{\sigma q}$ and $a_{j\delta q}$, equation (33), we get

$$i\phi_{r\sigma F}(x) + i\phi^\dagger_{r\sigma F}(x) = \sum_{j\delta q>0}\left(\lambda^{j\delta q}_{r\sigma F}(x)a_{j\delta q} - \lambda^{*j\delta q}_{r\sigma F}(x)a^\dagger_{j\delta q}\right).$$

In terms of $\Lambda^{j\delta}_{r\sigma}$, $B_{j\delta q}$ and $D_{j\delta q}$, cf. equations (34), (35) and (36), the coefficients $\lambda^{j\delta q}_{r\sigma F}(x)$ read

$$\lambda^{j\delta q}_{r\sigma F}(x) = \frac{\Lambda^{j\delta}_{r\sigma}}{\sqrt{n_q}}\left(e^{i\mathrm{sgn}(rF)qx}B_{j\delta q} - e^{-i\mathrm{sgn}(rF)qx}D_{j\delta q}\right). \quad (70)$$

By defining

$$\tilde{\lambda}^{j\delta q}_{[l]}(x) := -\tilde{\sum}_{n=1}^4\lambda^{j\delta q}_{l_n}(x) \quad (71)$$

and again using the Baker-Hausdorff formula, we arrive at

$$e^{-i\tilde{\sum}_{n=1}^4\left(\phi_{l_n}(x)+\phi^\dagger_{l_n}(x)\right)} = e^{-\sum_{j\delta q>0}\tilde{\lambda}^{*j\delta q}_{[l]}(x)a^\dagger_{j\delta q}}e^{\sum_{j\delta q>0}\tilde{\lambda}^{j\delta q}_{[l]}(x)a_{j\delta q}}e^{-\frac{1}{2}\sum_{j\delta q>0}\left|\tilde{\lambda}^{j\delta q}_{[l]}(x)\right|^2},$$

such that in total

$$\left\langle \boldsymbol{m}\left| e^{-i\tilde{\sum}_{n=1}^4\phi^\dagger_{l_n}(x)}e^{-i\tilde{\sum}_{n=1}^4\phi_{l_n}(x)}\right|\boldsymbol{m}'\right\rangle = A_{[l]}(x)\prod_{j\delta q}F(\tilde{\lambda}^{j\delta q}_{[l]}(x),m_{j\delta q},m'_{j\delta q}), \quad (72)$$

where we have introduced

$$A_{[l]}(x) := e^{\frac{1}{2}\left[i\tilde{\sum}_{n=1}^4\phi^\dagger_{l_n}(x),i\tilde{\sum}_{n'=1}^4\phi_{l_{n'}}(x)\right]} \times e^{-\frac{1}{2}\sum_{j\delta q>0}\left|\tilde{\lambda}^{j\delta q}_{[l]}(x)\right|^2}. \quad (73)$$

The function $F(\lambda,m,m') = \left\langle m\left|e^{-\lambda a^\dagger}e^{\lambda a}\right|m'\right\rangle$ is given by [6]

$$F(\lambda,m,m') = \left(\Theta(m'-m)\lambda^{m'-m} + \Theta(m-m')\left(-\lambda^*\right)^{m-m'}\right) \times \sqrt{\frac{m_{min}!}{m_{max}!}}\sum_{i=0}^{m_{min}}\frac{\left(-|\lambda|^2\right)^i}{i!(i+m_{max}-m_{min})!}\frac{m_{max}!}{(m_{min}-i)!}, \quad (74)$$

where $m_{min/max} = \min/\max(m, m')$. Combining (69) and (72) we finally obtain

$$M_{[l]}(\boldsymbol{m}, \boldsymbol{m}', x) = C_{[l]}(x) \times A_{[l]}(x) \prod_{j\delta q} F(\tilde{\lambda}^{j\delta q}_{[l]}(x), m_{j\delta q}, m'_{j\delta q}).$$

Explicitly, equation (73) yields that $A_{[l]}(x)$ only depends on the scattering type for the product rF. For $S_{rF} \neq u$ we find $A_{[l]_{S_{rF}}} =: A_{S_{rF}} \equiv 1$ whereas A_u is strongly enhanced leading to an increased importance of non-density-density interactions at half-filling. Due to its relevance we show the detailed calculation of A_u in the following.

B.2.1 Evaluation of A_u

As example we calculate $A_{[r]_{S_r}[F]_{S_F}[\sigma]_{S_\sigma}}$ with $(S_r, S_F, S_\sigma) = (b, f^-, f^+)$, i.e., for $[r] = (r, -r, r, -r)$, $[F] = (F, -F, -F, F)$ and $[\sigma] = (\sigma, \sigma, \sigma, \sigma)$. It is easily checked that for this choice $S_{rF} = u$ holds. Before starting with the actual calculation we first determine the coefficients $\tilde{\lambda}^{j\delta q}_{[r][F][\sigma]}(x)$ for the considered case. With equations (70) and (71) we find

$$\tilde{\lambda}^{j\delta q}_{[r]_b[F]_{f^-}[\sigma]_{f^+}}(x) = -\frac{1}{\sqrt{n_q}} \tilde{\sum}_{n=1}^{4} \Lambda^{j\delta}_{r_n\sigma_n} \left(e^{i\mathrm{sgn}(r_n F_n) qx} B_{j\delta q} - e^{-i\mathrm{sgn}(r_n F_n) qx} D_{j\delta q} \right).$$

The values for $B_{j\delta q}$, $D_{j\delta q}$ and $\Lambda^{j\delta}_{r\sigma}$ are known from the Bogoliubov transformation, cf. equations (34) to (36). For the different channels $j\delta$ this leads to

$$\tilde{\lambda}^{c+q}_{[r]_b[F]_{f^-}[\sigma]_{f^+}}(x) = -\frac{2i\mathrm{sgn}(rF)}{\sqrt{n_q}} \sqrt{\frac{\varepsilon_{0q}}{\varepsilon_{c+q}}} \sin(qx),$$
$$\tilde{\lambda}^{c-q}_{[r]_b[F]_{f^-}[\sigma]_{f^+}}(x) = 0$$
$$\tilde{\lambda}^{s+q}_{[r]_b[F]_{f^-}[\sigma]_{f^+}}(x) = -\frac{2i\mathrm{sgn}(rF\sigma)}{\sqrt{n_q}} \sin(qx),$$
$$\tilde{\lambda}^{s-q}_{[r]_b[F]_{f^-}[\sigma]_{f^+}}(x) = 0.$$

Using (73) we get in this case,

$$A_{[l]}(x) := e^{\frac{1}{2}\left[i\phi^\dagger_{l_1}(x) - i\phi^\dagger_{l_3}(x), i\phi_{l_1}(x) - i\phi_{l_3}(x)\right]} \times e^{\frac{1}{2}\left[i\phi^\dagger_{l_2}(x) - i\phi^\dagger_{l_4}(x), i\phi_{l_2}(x) - i\phi_{l_4}(x)\right]} \times e^{-\frac{1}{2}\sum_{q>0}\left(\left|\tilde{\lambda}^{c+q}_{[l]}(x)\right|^2 + \left|\tilde{\lambda}^{s+q}_{[l]}(x)\right|^2\right)}. \quad (75)$$

Improving readability we have again replaced the indices $rF\sigma$ by a single index l. With (42) we obtain

$$\left[i\phi^\dagger_{rF\sigma}(x), i\phi_{r\pm F\sigma}(x)\right] = -\sum_{q>0} \frac{1}{n_q} e^{-i\mathrm{sgn}(rF)q(x\mp x)} [b^\dagger_{\sigma r\cdot q}, b_{\sigma r\cdot q}] = \sum_{q>0} \frac{1}{n_q} e^{-i\mathrm{sgn}(rF)q(x\mp x)}.$$

In total this leads to

$$A_{[r]_b[F]_{f^-}[\sigma]_{f^+}}(x) := e^{2\sum_{q>0}\frac{1}{n_q}(1-\cos(2qx))} \times e^{-2\sum_{q>0}\frac{1}{n_q}\left(\frac{\varepsilon_{0q}}{\varepsilon_{c+q}}+1\right)\sin^2(qx)}.$$

Because of $\sin^2(qx) = \frac{1}{2}(1 - \cos(2qx))$ the final result is

$$A_{[r]_b[F]_{f^-}[\sigma]_{f^+}}(x) := e^{2\sum_{q>0}\frac{1}{n_q}\left(1-\frac{\varepsilon_{0q}}{\varepsilon_{c+q}}\right)\sin^2(qx)}. \quad (76)$$

The same result is also obtained for all other processes with $S_{rF} = u$.

C Regularization of $\langle \boldsymbol{Nm} | V_{f^+ b f^-} | \boldsymbol{Nm} \rangle$

As already mentioned in the main text, expression (50) for the matrix element $\langle \boldsymbol{Nm} | V_{S_r S_F S_\sigma} | \boldsymbol{N'm'} \rangle$ diverges if $\sum_{j\delta q} \left| m_{j\delta q} - m'_{j\delta q} \right| \leq 1$ and if $V_{S_r S_F S_\sigma}$ is $\boldsymbol{N}$ conserving. Here we show in detail how the matrix element can be properly regularized for the case $\boldsymbol{m} = \boldsymbol{m}'$ and $V_{S_r S_F S_\sigma} = V_{f^+ b f^-}$. We start with equation (50),

$$\langle \boldsymbol{Nm} | V_{f^+ b f^-} | \boldsymbol{Nm} \rangle = \frac{1}{4L} u^+ \sum_{rF\sigma} \int dx \frac{e^{-2i\mathrm{sgn}(rF)(N_{r\sigma} - N_{r-\sigma})\frac{\pi}{L}x}}{4\sin^2\left(\frac{\pi}{L}x\right)} \times \prod_{j\delta q} F(\tilde{\lambda}^{j\delta q}_{[r]_{f^+}[F]_b[\sigma]_{f^-}}(x), m_{j\delta q}, m_{j\delta q}). \quad (77)$$

In a first step we rewrite the fraction $\frac{e^{-2i\mathrm{sgn}(rF)(N_{r\sigma} - N_{r-\sigma})\frac{\pi}{L}x}}{4\sin^2(\frac{\pi}{L}x)}$ as $\frac{e^{-2i\mathrm{sgn}(rF)N_{r\sigma}\frac{\pi}{L}x}}{1-e^{i\frac{2\pi}{L}x}} \frac{e^{2i\mathrm{sgn}(rF)N_{r-\sigma}\frac{\pi}{L}x}}{1-e^{-i\frac{2\pi}{L}x}}$ and, by using the identity

$$\sum_{n=-\infty}^{N} e^{-inx} = \frac{e^{-iNx}}{1-e^{ix}},$$

we transform it into the product of two infinite sums extending over the whole Fermi sea,

$$\frac{e^{-2i\mathrm{sgn}(rF)(N_{r\sigma} - N_{r-\sigma})\frac{\pi}{L}x}}{4\sin^2(\frac{\pi}{L}x)} = \sum_{n=-\infty}^{N_{r\sigma}} e^{-2i\mathrm{sgn}(rF)n\frac{\pi}{L}x} \sum_{n'=-\infty}^{N_{r-\sigma}} e^{2i\mathrm{sgn}(rF)n'\frac{\pi}{L}x}. \quad (78)$$

An important observation is, that the multiplication with $e^{-in_q x} - e^{in_q x} = e^{-in_q x}\left(1 - e^{2in_q x}\right)$ recasts the infinite sum $\sum_{n=-\infty}^{N} e^{-2inx}$ into a finite sum,

$$e^{-in_q x}\left(1 - e^{2in_q x}\right) \sum_{n=-\infty}^{N} e^{-2inx} = e^{-in_q x} \sum_{n=N-n_q+1}^{N} e^{-2inx}. \quad (79)$$

We now have a closer look at the coefficients $\tilde{\lambda}^{j\delta q}_{[r]_{f^+}[F]_b[\sigma]_{f^-}}$, which according to (71) are given by

$$\tilde{\lambda}^{j\delta q}_{[r]_{f^+}[F]_b[\sigma]_{f^-}}(x) = \frac{1}{\sqrt{n_q}}\left[\Lambda^{j\delta}_{r\sigma}\left(e^{-i\mathrm{sgn}(rF)qx} - e^{i\mathrm{sgn}(rF)qx}\right) + \Lambda^{j\delta}_{r-\sigma}\left(e^{i\mathrm{sgn}(rF)qx} - e^{-i\mathrm{sgn}(rF)qx}\right)\right].$$

Then because of (79), the product

$$\prod_{j\delta q}\left(\tilde{\lambda}^{j\delta q}_{[r]_{f^+}[F]_b[\sigma]_{f^-}}(x)\right)^{t_{j\delta q}} \times \sum_{n=-\infty}^{N_{r\sigma}} e^{-2i\mathrm{sgn}(rF)n\frac{\pi}{L}x} \sum_{n'=-\infty}^{N_{r-\sigma}} e^{2i\mathrm{sgn}(rF)n'\frac{\pi}{L}x},\ r_{j\delta q}\in\mathbb{N}$$

is a finite sum for $\sum_{j\delta q} t_{j\delta q} \geq 2$. But from (74) we can conclude that

$$\prod_{j\delta q} F(\tilde{\lambda}^{j\delta q}_{[r]_{f^+}[F]_b[\sigma]_{f^-}}(x), m_{j\delta q}, m_{j\delta q}) = 1 + \mathcal{O}(\lambda^2),$$

where $\mathcal{O}(\lambda^2)$ collects all those terms which contain a factor $\prod_{j\delta q}\left(\tilde{\lambda}^{j\delta q}_{[r]_{f^+}[F]_b[\sigma]_{f^-}}(x)\right)^{t_{j\delta q}}$ with $\sum_{j\delta q} t_{j\delta q} \geq 2$. Thus

$$\int dx \frac{e^{-2i\mathrm{sgn}(rF)(N_{r\sigma}-N_{r-\sigma})\frac{\pi}{L}x}}{4\sin^2\left(\frac{\pi}{L}x\right)} \times \left(\prod_{j\delta q} F(\tilde{\lambda}^{j\delta q}_{[r]_{f^+}[F]_b[\sigma]_{f^-}}(x), m_{j\delta q}, m_{j\delta q}) - 1\right) \quad (80)$$

is a well defined integral over a finite sum and therefore not diverging. On the other hand we find with (78)

$$\int dx \frac{e^{-2i\mathrm{sgn}(rF)(N_{r\sigma}-N_{r-\sigma})\frac{\pi}{L}x}}{4\sin^2\left(\frac{\pi}{L}x\right)} = \int dx \sum_{n=-\infty}^{N_{r\sigma}} e^{-2i\mathrm{sgn}(rF)n\frac{\pi}{L}x} \sum_{n'=-\infty}^{N_{r-\sigma}} e^{2i\mathrm{sgn}(rF)n'\frac{\pi}{L}x} = L\sum_{n=-\infty}^{N_{r\sigma}}\sum_{n'=-\infty}^{N_{r-\sigma}} \delta_{n,n'} = \sum_{n=-\infty}^{\min(N_{r\sigma},N_{r-\sigma})} L.$$

Regularization of the previous expression now is easily achieved by subtracting in the previous equation e.g. the contribution from below half-filling, such that,

$$\int dx \frac{e^{-2i\mathrm{sgn}(rF)(N_{r\sigma}-N_{r-\sigma})\frac{\pi}{L}x}}{4\sin^2\left(\frac{\pi}{L}x\right)} = L\min(N_{r\sigma}, N_{r-\sigma}). \quad (81)$$

Combining (80) and (81) we obtain the finite expression,

$$\left\langle \boldsymbol{Nm}\left|V_{f^+bf^-}\right|\boldsymbol{Nm}\right\rangle = u^+\sum_r \min(N_{r\uparrow}, N_{r\downarrow}) + \frac{1}{4L}u^+\sum_{rF\sigma}\int dx \frac{e^{-2i\mathrm{sgn}(rF)(N_{r\sigma}-N_{r-\sigma})\frac{\pi}{L}x}}{4\sin^2\left(\frac{\pi}{L}x\right)} \times \left(\prod_{j\delta q} F(\tilde{\lambda}^{j\delta q}_{[r]_{f^+}[F]_b[\sigma]_{f^-}}(x), m_{j\delta q}, m_{j\delta q}) - 1\right),$$

which is equivalent to equation (51) in the main text. The regularization for the case $\sum_{j\delta q}\left|m_{j\delta q} - m'_{j\delta q}\right| = 1$ as well as for the matrix elements of the $\boldsymbol{N}$ conserving processes V_{f^-bf} and $V_{bf^-f^+}$ which are only relevant near half-filling can be achieved in a similar way.

References

1. R. Egger and A. O. Gogolin, Phys. Rev. Lett. **79**, 5082 (1997); Eur. Phys. J. B **3**, 281 (1998).
2. H. Yoshioka, A. A. Odintsov, Phys. Rev. Lett. **82**, 374 (1999).
3. M. Bockrath *et al.*, Nature **397**, 598 (1999).
4. H. W. Ch. Postma *et al.*, Science **293**, 76 (2001).
5. C. Kane, L. Balents and M. P. A. Fisher, Phys. Rev. Lett. **79**, 5086 (1997).
6. L. Mayrhofer, M. Grifoni, Phys. Rev. B **74**, 121403(R) (2006); Eur. Phys. J. B **56**, 107 (2007).
7. W. Liang, M. Bockrath and H. Park, Phys. Rev. Lett. **88**, 126801 (2002).
8. S. Sapmaz *et al.*, Phys. Rev. B **71**, 153402 (2005).
9. S. Moriyama, T. Fuse, M. Suzuki, Y. Aoyagi, K. Ishibashi, Phys. Rev. Lett. **94**, 186806 (2005).
10. Y. Oreg, K. Byczuk and B. I. Halperin, Phys. Rev. Lett. **85**, 365 (2000).
11. E. Lieb and D. Mattis, Phys. Rev. **125**, 164 (1962).
12. For the other types of metallic nanotubes only the magnitudes of the effective 1D interaction potentials change marginally, see, A. A. Odintsov and H. Yoshioka, Phys. Rev. B **59**, R10457 (1999).
13. D. P. DiVincenzo and E. J. Mele, Phys. Rev. B **29**, 1685 (1984).
14. J. Jiang, J. Dong and D. Y. Xing, Phys. Rev. B **65**, 245418 (2002).
15. W. Barford, *Electronic and Optical Properties of Conjugated Polymers*, (Clarendon Press, Oxford, 2005).
16. P. Fulde, *Electron Correlations in Molecules and Solids* (Springer Verlag, Berlin - New York, 1995).
17. For an introduction to bosonization, see e.g., J. v. Delft, H. Schoeller, Annalen Phys. **7**, 225 (1998).
18. J. Avery, *Creation and Annihilation Operators* (McGraw-Hill, New York, 1976)
19. M. Eto and Y. V. Nazarov, Phys. Rev. Lett. **85**, 1306 (2000); Phys. Rev. B **66**, 153319 (2002).